1973

Electrophysiologic Studies Of Osteoblasts.

Billie Gail Griggs Jeansonne
University of Alabama at Birmingham

ELECTROPHYSIOLOGIC STUDIES OF OSTEOBLASTS

by

BILLIE GAIL GRIGGS JEANSONNE

A DISSERTATION

Submitted in partial fulfillment of the requirements for the degree of Doctor of Philosophy in the Department of Physiology and Biophysics in The Graduate School of the University of Alabama in Birmingham

BIRMINGHAM, ALABAMA

1973

ACKNOWLEDGEMENTS

I thank my advisors, Drs. F. F. Feagin and R. L. Shoemaker for their academic guidance during the entire course of my graduate studies, and particularly during the execution of the experiments reported herein.

I thank Dr. Rehm for his help with electrophysiologic techniques and interpretations.

Last, but certainly not least, I thank my husband for his help and encouragement in my work, both at school and at home.

DEDICATION

"..... the inherently curious: the clinician who wonders why, the anatomist who wonders where, the chemist who wonders how, and just any investigator who wonders whether."

W. F. and M. W. Neuman

TABLE OF CONTENTS

Table of Contents (continued)

LIST OF TABLES

LIST OF FIGURES

LIST OF PLATES

CHAPTER 1

INTRODUCTION TO BONE RESEARCH

Bone is a rigid connective tissue which serves a dual role as a supporting structure and as a reservoir of body calcium. Bone is formed by osteoblasts which produce the organic matrix (mainly collagenous) in which calcium apatite crystals are embedded. These calcium apatite crystals form from serum calcium and give bone its rigidity for structural support of the body. To serve as a reservoir of body calcium these same minerals must be available to replenish serum calcium whenever necessary.

The support function of bone is controlled directly by the bone cells which involve themselves in apposition and resorption of bone tissue. In bone apposition and resorption the minerals are derived from or added to the calcium of serum. Thus, control of the support function may affect serum calcium homeostasis. Conversely, the level of serum calcium is regulated by parathyroid hormone (PTH) and thyrocalcitonin (TCT). These hormones also affect the rates of apposition and resorption of bone tissue. Thus, the two functions of bone are intimately associated through the minerals of bone which they both involve. The need for integration of control of both functions is obvious.

The problem of bone-serum interaction is magnified by the fact that serum is supersaturated with respect to the growth of apatite mineral crystals, but undersaturated with respect to the formation of new crystals (31). Historically, this fact guided the formation of theories of calcification for over fifty years. Assuming an ionic composition of the extracellular fluid in contact with the calcifying osteoid to be similar to serum, theories were proposed for the mechanism of induction of the first micro-crystals of apatite which could then grow in this fluid. Two mechanisms are possible: 1) the ionic composition of the fluid is altered to exceed the critical ion product for apatite precipitation, or 2) the first micro-crystals are formed under the guidance of the organic matrix which orients the ions properly for crystal formation. Both of these mechanisms imply indirect cellular control, by the production of enzymes or of a specific organic matrix component.

Only recently has a more direct cellular control of the minerals of bone been seriously considered. As early as 1956, Howard (19) proposed that the minerals of bone are separated from the rest of the body by an envelope of cells. However, this proposal was generally ignored at the time.

With the demonstration that the hormonal regulation of serum calcium levels occurs too rapidly to be accounted for by osteoclastic activity, other regulators of calcium movement were sought. Morphologic changes in the perilacunar matrix in parathyroid hormone-treated animals indicated that osteocytes could engage in

both removal (osteolysis) and deposition (osteoplasis) of bone matrix (2). Osteoblasts were demonstrated to respond to PTH and to increased medium calcium levels with increased RNA synthesis (34, 35). This led Talmage to propose that PTH exerts its effects on bone primarily through the osteocytes (42) and osteoblasts (43).

The studies by Baud (2) gave morphologic evidence for a continuous layer of cells - osteoblasts, osteocytes, and pericapillary lining cells - that almost completely enveloped the bone mineral. On the basis of his finding of a high potassium concentration in the fluids of bone, Neuman and co-workers (10, 16, 45) proposed a bone-blood barrier separating the bone extracellular fluid from the general extracellular fluid of the body. Possibly the cellular envelope described by Baud serves as this barrier.

Extending the theory of cellular control of mineral activity, Vitalli (47) proposed that the osteocyte-osteoblast cells comprise an independent servo control feedback system for calcium, whose level of activity is determined by PTH. Rasmussen and co-workers (37) added their evidence from metabolic activities of cells in response to PTH and/or calcium to support the idea that bone cells respond primarily to cytoplasmic calcium concentrations and to PTH through its effect of increasing the influx of calcium into the cytoplasm.

Borle's studies of the calcium ion movements in cultured HeLa and kidney cells make this a very tenable proposal. His studies showed that calcium influx into the cytoplasm is passive (6),

while efflux from the cytoplasm into the extracellular fluid or mitochondria is an active process (7). In this same system, PTH increases passive influx which then affects efflux rates (5), while TCT increases the active efflux from the cytoplasm into the mitochondria and inhibits the active efflux of calcium from cytoplasm to the extracellular fluid (8). These studies did not define the efflux from cytoplasm into the mitochondria. Based on the knowledge that isolated mitochondria can accumulate calcium ions in concentrations greater than 1000 times that of the bathing solution (14) and on the quantitative and qualitative similarities between his system and isolated mitochondria (23), he proposed that mitochondria were the active subcellular compartment in his cell systems that accounted for the observed rise in total cell calcium (9).

The mitochondrial accumulations of calcium and phosphate were proposed by Lehninger (23) to serve as the nucleus for calcification. He proposed that mitochondrial minerals were packaged, possibly by mitochondrial membrane lipids, and extruded intact by some unknown mechanism into the calcifying matrix. This mitochondrial lipid could be the same lipid of the calcifying front described by Irving and Wuthier (20) to be directly involved in the calcification process, possibly as a nucleating template.

However, Bonucci (4) has postulated that thin proteic filaments which he calls "crystal ghosts" serve as the template for the apatite crystals. It is possible that the lipids serve to

transport the packaged minerals to the proteic filaments which guide their growth.

By whatever means the calcification process is initiated, the growth of the crystals depends on the availability of calcium ions to the calcifying front. Also, there must be a pathway by which ions may travel to and from bone during osteocytic osteolysis and osteoplasis. Baud (2) proposed that the perilacunar matrix served as an extracellular path for such ion movements.

More recent morphologic studies (18, 48), have defined a possible intracellular route for such ion movements through cytoplasmic processes, across tight junctions, from one cell to another. In this manner, all cells of bone form a functional syncytium to make available (to the serum) vast stores of calcium in the fluid of bone.

The growing interest in and evidence for the important role bone cells, osteoblasts particularly, play in calcium movement and homeostasis is indirect. The purpose of this work is to study this role of osteoblasts in calcium movements by studies on the osteoblasts themselves in situ.

Four experimental objectives were outlined, the results of which would serve to define the role of osteoblasts in calcium movements:

1) The resting transmembrane potential of osteoblasts and its responses to changes in the ionic composition of the bathing solution and to a hormone (TCT) would be determined in order to

define the role of these ions in transmembrane processes and the effect of TCT on these processes.

2) The intracellular injection of dye and the observation of its movements would be performed to test the physiologic significance of the tight junction between the cells.

3) Electrical coupling between osteoblasts would be tested to confirm the results of the dye injection experiments.

4) The calvaria as a sheet of tissue would be studied in a system that allowed determination of its membrane properties.

Each of the preceding objectives is pursued independently in the succeeding four chapters.

CHAPTER 2

TRANSMEMBRANE POTENTIALS OF OSTEOBLASTS

Intracellular recordings of animal cells were introduced independently in 1939-40 by Cole and Curtis (11) in the United States and Hodgkin and Huxley (17) in England. They used large (100 micron diameter) electrodes developed for extracellular recordings, but in the squid giant axon. Studies of the membrane potentials of the smaller mammalian cells was not possible until 1949 when glass microelectrodes were developed (25).

Since that time the transmembrane potentials of many mammalian cells have been recorded. Such studies have greatly expanded our knowledge of ionic movements and membrane properties associated with such movements.

Conspicuous by their absence are recordings from connective tissue cells. The morphology of these tissues (cells embedded in large matrix) makes the cells difficult targets for the fragile microelectrodes. Also, these cells were not generally considered to be excitable, nor secretory or absorptive. Thus, these cells were disregarded in favor of technically easier, more fruitful studies of other cells. However, with the recent increased interest in the

role of bone cells in calcium ion regulation, studies of the membrane properties of osteogenic cells are now needed.

Only two studies dealing with the transmembrane potentials of connective tissue cells have been reported. In one study, the transmembrane potentials of canine and human odontoblasts were recorded *in situ* both *in vivo* and *in vitro* (49). The average membrane potential was 30 mV, inside negative. In the other study, the membrane potentials of osteoclasts were recorded on normal isolated cells, and on isolated cells treated with TCT or PTH (29). The untreated cells had an average transmembrane potential of 17.3 mV, inside negative, with a bimodal distribution with peaks at 9.6 and 22.7 mV. Measurements on osteoclasts exposed to PTH corresponded to the lower peak while those exposed to TCT corresponded to the higher peak.

To my knowledge, no studies have been made of osteoblasts, or of the membrane responses to changes in ionic composition of the bathing medium on any osteogenic or odontogenic cells. In this study such responses are recorded in view of defining some basic parameters of the membrane characteristics of osteoblasts.

Methods and Procedures

Six female albino rats with litters of 24-day old pups were obtained. Each female had 8 to 10 pups of which 4 were used for *in vitro* recordings of transmembrane potentials of osteoblasts on the surface of the parietal bones. The rats were obtained at

specific intervals of time to insure that no more than two experiments were performed on any one day.

For each experiment, a pup from the designated litter was sacrificed by decapitation and the scalp removed to expose the calvarium. The calvarium was then excised, taking care not to damage the parietal bones. The excised tissue was placed in a petri dish filled with Hank's balanced salt solution (Hank's BSS) (36). The preparation and composition of all Hank's BSS's are given in Appendix 1. The periosteum was carefully stripped from the outer surface of the bone with forceps, and the surface gently wiped with a lint-free tissue.

The stripped calvarium was tied to a flat stainless steel ring with silk thread, then stained by immersion for approximately 5 minutes in 30 ml of a 0.25% solution (w/v) of Niagara Sky Blue 6B* in Hank's BSS. In this manner, staining was minimal, but sufficient to allow good microscopic visualization of individual cells.

The tissue was then placed in a shallow circular Lucite chamber (figure 1) filled with 12 ml of Hank's BSS. The tissue on the stainless steel ring was firmly anchored in the chamber, by means of nuts, to bolts sealed in the bottom of the chamber and fitted through holes in the stainless steel ring.

Microelectrodes were prepared from 9-cm lengths of glass capillary tubing, 1.2 to 1.4 mm outer diameter. The capillaries

---

*National Biological Stains and Reagents, Morristown, New Jersey.

Figure 1. Chamber for Calvaria Used for Transmembrane Potential Recordings: A small volume (15 ml) clear plastic chamber is fitted with a stainless steel ring, to which the calvarium is tied, that can be anchored in the chamber by means of nuts to bolts sealed in the bottom of the chamber and fitted through holes in the stainless steel ring. A silver-silver chloride wire is sealed in the chamber to complete the current circuit for dye injection and electrical coupling experiments.

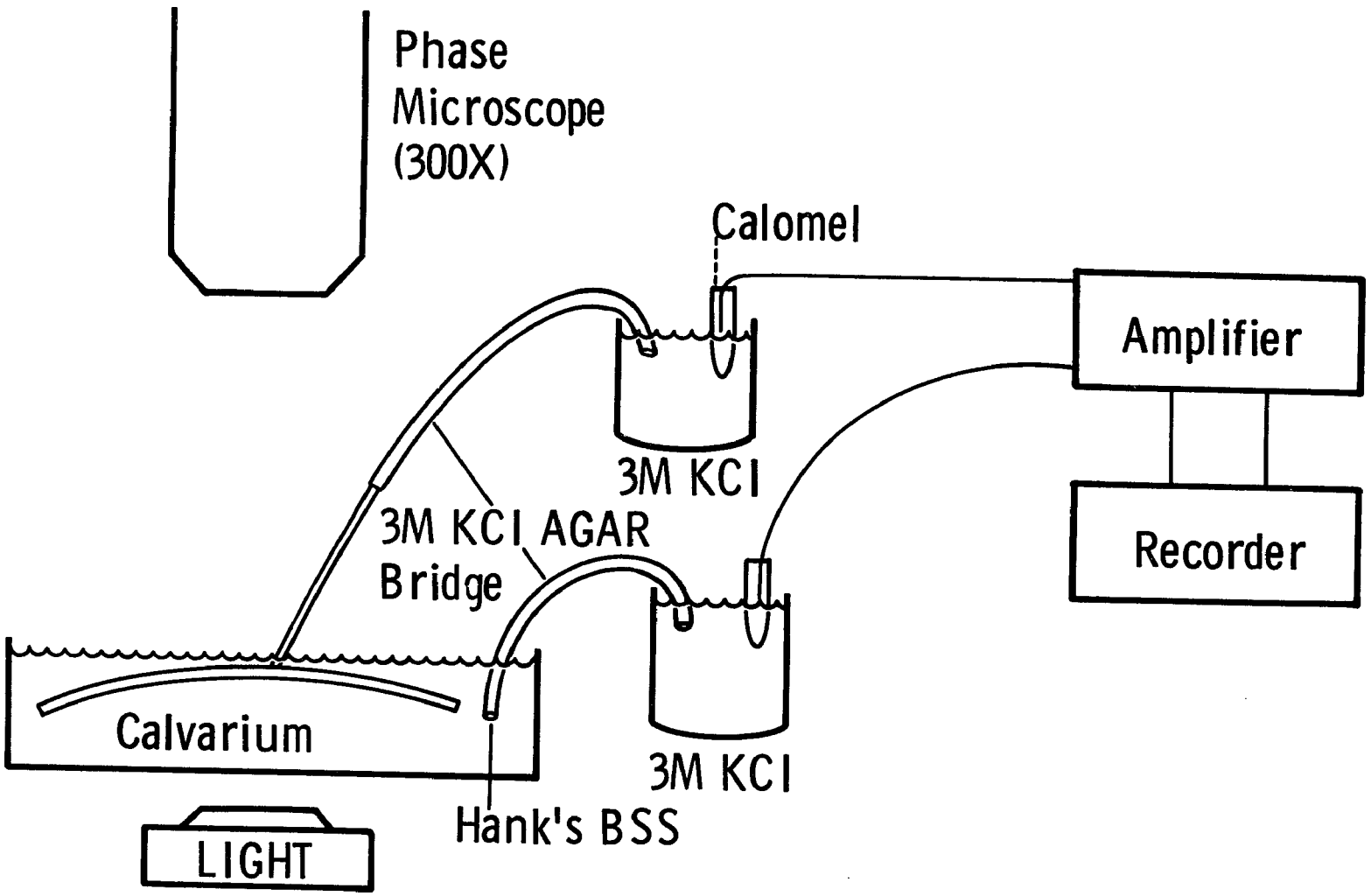
Phase
Microscope
(300X)
Calomel
Amplifier
3M KCl
3M KCl AGAR
Bridge
Recorder
Calvarium
3M KCl
Hank's BSS
LIGHT

were cleaned by washing in saturated Alconox solution (75°C), then rinsing 8 to 10 times in distilled water and 4 or 5 times in acetone. The clean capillaries were dried overnight in an oven at 40°C, and stored in a clean, covered petri dish.

Each length of the capillary tubing was pulled on a horizontal, solenoid-type micropipette puller into two micropipettes with tips less than one micron in diameter (25). Twelve micropipettes were pulled and secured to a glass microscopic slide by rubber bands to protect the tips during subsequent handling. The tips of the micropipettes were checked microscopically for approximate size and final taper. The micropipettes were either filled immediately or stored dry for not more than one week in a plastic film-sealed vacuum flask.

The micropipettes were filled with absolute methanol by boiling under vacuum, then equilibrated for 30 minutes with distilled water before final equilibration with filtered 3 M KCl for at least 4 hours, usually overnight. The filled microelectrodes were used within one week of filling, after which time the tip resistances became erratic and the recording properties unstable due to obvious crystal formation within the tips.

Only microelectrodes with tip potentials of less than 5 mV, and tip resistances of 10 to 50 MΩ were used in any experiment.

The set-up for transmembrane potential recording (40, 41) is illustrated in figure 2. The microelectrode was connected by a 3 M KCl agar bridge and calomel electrode to a high impedance

Figure 2. Transmembrane Potential Recording Set-Up: A micro-electrode is connected by a 3 M KCl agar bridge and calomel electrode to a high impedance amplifier and a mV recorder. The circuit is completed by a second 3 M KCl agar bridge and calomel electrode from the solution in the tissue chamber to ground on the amplifier and recorder.

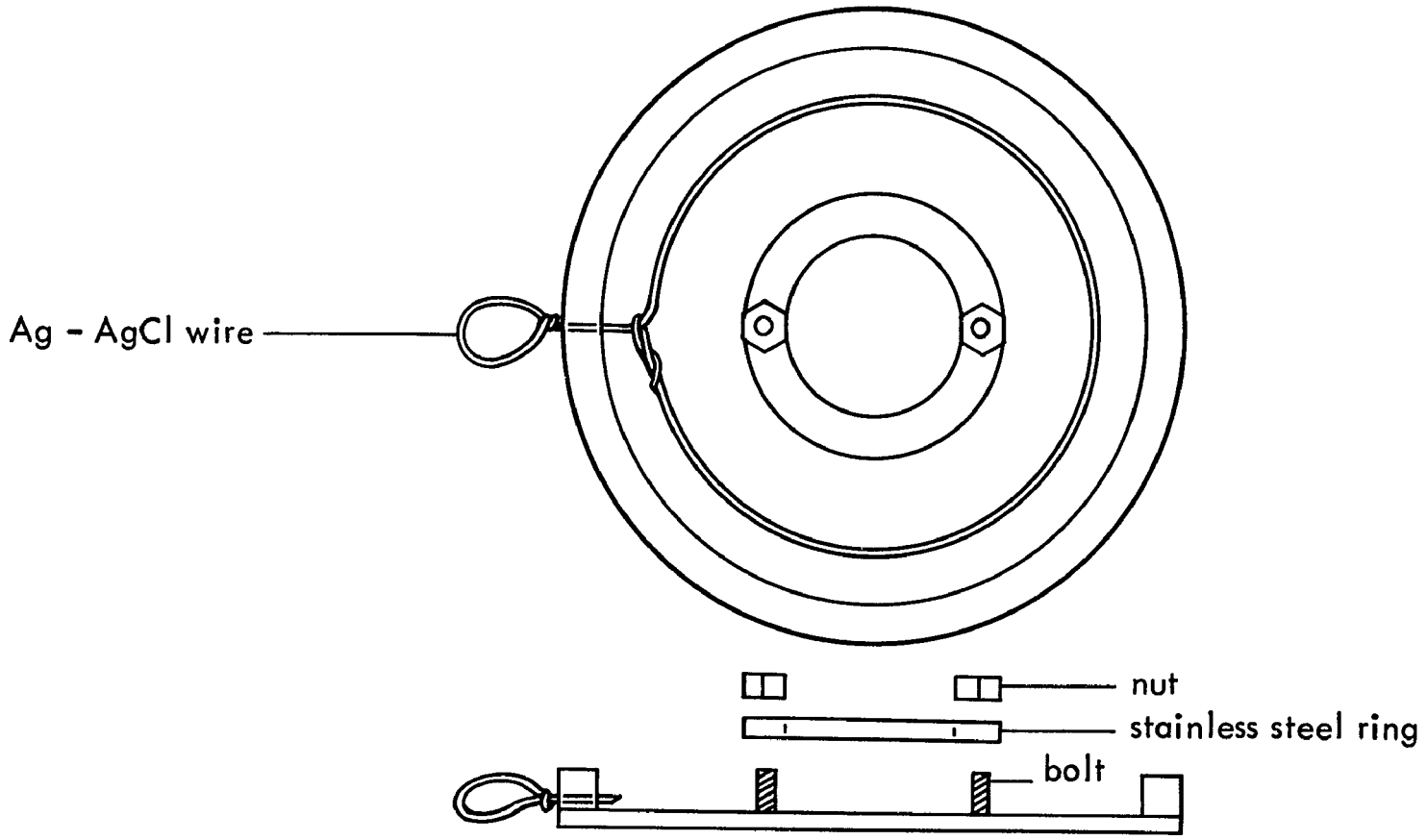
Ag - AgCl wire
nut
stainless steel ring
bolt

electrometer* and a mV recorder. Zero ground reference for the recording circuit was made by a second 3 M KCl agar bridge and calomel electrode from the solution in the tissue chamber to ground on the electrometer and recorder.

The potential of the calomel electrodes was nulled to zero by a balancing voltage. Then the microelectrode was inserted in the 3 M KCl agar bridge, attached to the micromanipulator, and lowered into the solution in the chamber. The microelectrode tip potential was nulled by a balancing voltage.

The microelectrode tip and the tissue in the chamber were viewed with a phase microscope at 300 X magnification. The microelectrode was placed inside a cell, under microscopic visualization, by means of a mechanical micromanipulator.

Recordings were acceptable if the tip resistance did not change by more than 2 mV (or half of the recorded potential, whichever was less) before, during, or after the recording period, and if the transmembrane potential was stable for at least 30 seconds. Ten to twelve recordings were made of the transmembrane potentials of osteoblasts on each animal. All recordings were obtained within 3 hours of the time the pup was sacrificed.

For experiments in which changes of the bathing solution were made, a different chamber was used (figure 3). This chamber has a smaller total volume of 6 to 8 ml to allow more rapid exchange of

---

*W-P Instruments, Inc., Hamden, Connecticut. Model M4A Electrometer.

Figure 3. Chamber for Calvaria Used for Solution Changes: A small volume (6-8 ml) clear plastic chamber is fitted with a stainless steel ring, to which the calvarium is tied, that can be anchored in the chamber by means of nuts to bolts which are sealed in the bottom of the chamber and fitted through holes in the stainless steel ring. Stainless steel inlet and outlet ports, from which tubing projects around the inner circumference of the chamber, are connected to syringes used for the solution changes.

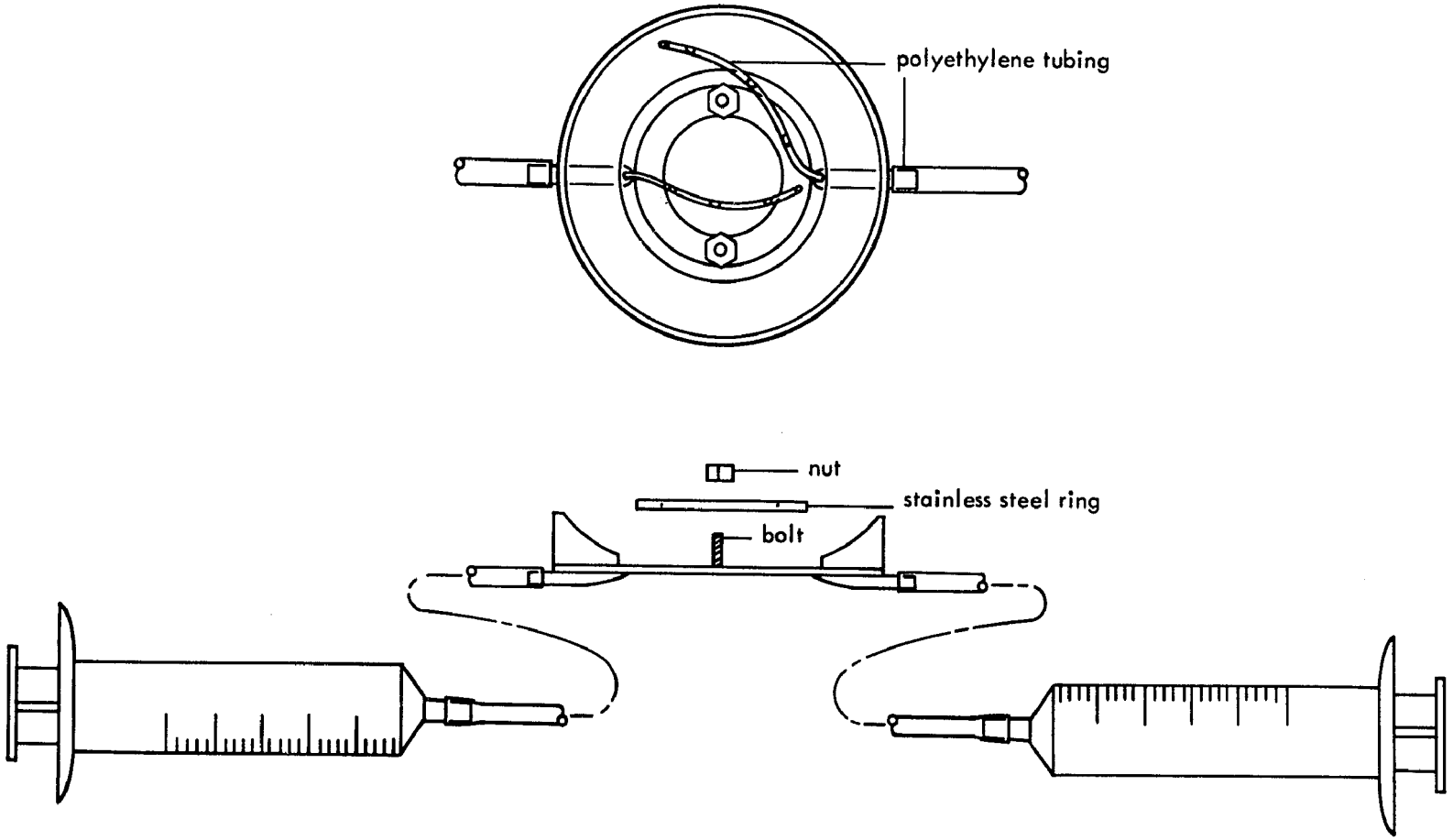
polyethylene tubing
nut
stainless steel ring
bolt

the solutions. Polyethylene tubing with six holes at various sites along its length was inserted into the inlet and outlet ports and arranged around the inner circumference of the chamber. Preliminary tests with dye solutions showed rapid and complete mixing and exchange of the solutions. Changes of solutions were accomplished by two manually operated syringes fitted to the inlet and outlet ports by polyethylene tubing. The experimental solution was injected into the chamber from one syringe and the control solution simultaneously aspirated into the second syringe.

In 29 experiments on 14 pups from 3 litters, the responses of the transmembrane potential to changes in the bathing solution were recorded. In each experiment a 30 second period of stable control transmembrane potential was recorded prior to the initiation of solution exchange. Then, with continuous monitoring of the transmembrane potential, 20 ml of the experimental solution were injected into the chamber (and the excess simultaneously aspirated) in two minutes. The same experimental recording set-up and criteria of acceptability were employed in these experiments as in the previous transmembrane potential experiments. Additionally, the recording was acceptable only if it remained stable for at least 30 seconds after completion of the solution exchange. Between each two experiments, the chamber, syringes, and all tubing were rinsed thoroughly with standard Hank's BSS.

Those experimental solutions used were low sodium, high potassium, chloride-free, calcium-free, fluoride, and thyrocalcitonin

(TCT) Hank's BSS's. Appendix 1 contains the details of preparation and composition of all of these solutions.

Additional control experiments were performed for each solution using the same procedure except that the microelectrode was placed near the surface of the tissue, not within a cell. This allowed observation of changes in zero-potential baseline caused by the exchange of solutions.

In vivo recordings of transmembrane potentials were performed on three 10- or 11-day old pups, all from the same litter. The pups were anesthetized with Nembutal (3 mg/kg body weight in a 1% solution injected intraperitoneally) and the parietal bones exposed by removing the scalp from a small area. The periosteum of the exposed bone was carefully stripped, and the wound filled with Hank's BSS (about 1 ml). A second small incision was made through the scalp near the exposed area of bone. A 3 M KCl agar bridge was inserted through this hole to contact the fluid in the wound. The animal was placed on the stage of the microscope and the 3 M KCl agar bridge was connected to the ground reference calomel electrode.

The electrical recording set-up was the same as that used for in vitro recordings, with the same criteria of acceptability. Visualization of individual cells was not possible in these experiments; the microscope stage was used strictly as a convenient animal holder. Verification of transmembrane potentials was made by the lack of change of tip resistance throughout each recording period.

The data from experiments in which transmembrane potentials were recorded on pups of different litters at various ages were subjected to an Analysis of Variance for statistical differences with litters or ages.

Results

The transmembrane potentials obtained *in vitro* are shown in Table 1. A total of 248 recordings from 10 to 12 cells on each of 24 3- to 24-day old pups were made. The overall mean transmembrane potential was 3.93 mV, with the inside of the cell negative to the bathing solution. The standard error was ±0.361. The means and standard errors for each age were 4.02 ± 0.393, 4.23 ± 0.519, 3.79 ± 0.334, and 3.65 ± 0.583 at 3, 10, 17 and 24 days, respectively.

The analysis of variance (Table 2) shows no significant variation (> 0.5) with age in the range of ages studied. There was, however, a < 0.06 level of significance for litters and age, due entirely to the highly significant litter variation (< 0.02).

The responses of transmembrane potentials to changes of sodium, potassium, fluoride, and calcium concentrations in the bathing solutions are given in Tables 3 and 4. The response to low sodium was a hyperpolarization of 0.5 to 1.0 mV. The time course of hyperpolarization and the occurrence of recovery were variable. The response to high potassium was that of a depolarization of 0.5 to 1.0 mV with variable time course and recovery. These results with

Table 1. *In Vitro* Transmembrane Potentials (mV) of Osteoblasts

Age	Litters 1	2	3	4	5	6	n	Mean	±S.E.
3 days	5.0*	1.5	2.5	1.0	3.5	1.5	63	4.02	0.393
	5.5	3.0	2.0	3.0	4.5	6.0			
	2.0	7.0	4.0	3.5	2.0	2.5			
	7.0	5.0	3.0	4.5	3.5	2.5			
	8.0	3.5	4.5	3.5	5.0	5.5			
	2.5	1.5	1.0	6.0	2.0	4.0			
	7.0	12.0	1.5	8.5	2.0	2.0			
	8.0	5.0	1.0	2.0	3.5	6.0			
	1.5	14.0	2.0	1.5	1.0	7.0			
	3.5	3.0	9.5	2.0	3.0	5.5			
		2.0		2.5					
				4.0					
10 days	9.0	3.0	4.5	3.0	4.5	4.0	64	4.23	0.519
	6.0	2.5	2.5	2.0	2.0	4.5			
	7.5	2.0	1.0	6.0	5.0	1.5			
	12.0	3.5	4.0	8.0	2.5	1.5			
	7.0	6.0	4.0	6.0	4.0	7.0			
	5.0	6.5	1.0	5.0	3.0	3.0			
	6.0	2.5	3.5	1.0	5.0	1.5			
	3.0	3.0	3.0	2.5	3.5	1.5			
	7.0	10.5	3.0	4.0	6.5	4.5			
	5.0	4.5	4.0	6.0	2.0	1.0			
	5.0	3.5	4.0			5.0			
17 days	3.0	4.0	2.0	7.5	4.0	3.5	60	3.79	0.334
	0.5	7.5	4.0	6.0	4.0	3.5			
	3.5	2.5	1.5	3.5	4.0	2.5			
	8.5	3.5	3.0	4.5	6.0	1.0			
	7.0	5.5	4.5	1.0	1.0	1.5			
	7.0	1.5	2.0	4.0	2.0	2.5			
	2.5	5.5	3.0	2.5	3.5	2.0			
	7.0	4.5	4.5	3.5	4.5	6.0			
	5.5	6.0	1.5	4.5	4.0	3.5			
	4.5	4.0	2.5	1.0	5.5	3.0			
24 days	3.0	2.5	3.0	1.0	1.5	10.0	61	3.65	0.583
	5.5	1.5	1.0	5.0	1.5	2.5			
	4.0	1.5	3.0	5.0	3.5	4.0			
	7.5	3.0	3.5	3.0	4.0	9.5			
	5.5	3.0	1.0	5.5	10.0	3.5			
	3.5	1.0	4.5	2.0	2.5	5.0			
	2.5	2.0	3.5	2.0	0.5	3.0			
	6.5	2.5	1.0	4.5	3.0	3.5			
	7.5	3.5	1.0	4.0	1.5	5.5			
	9.0	2.5	1.5	4.0	2.5	7.0			
		2.0							
Overall							248	3.93	0.361

*Each recording is from a different cell. Ten to twelve recordings were made on each animal, from each litter at each age.

Table 2. Analysis of Variance of *in Vitro* Transmembrane Potentials*

Source	d.f.	s.s.	m.s.	F-Ratio	Significance Level
Litters	5	161.8085	32.3617	4.30	< 0.02
Age - linear	1	7.4206	7.4206	0.99	> 0.50
Age - nonlinear	2	4.7045	2.3523	0.31	> 0.70
Litters X Age	15	112.8690	7.5246	1.67	< 0.06
Within Pups	224	1009.8909	4.5084		
Total	247	1296.6935			

*Analysis of data presented in Table 1.

Table 3. Responses of Transmembrane Potentials of Osteoblasts to Changes of Sodium and Potassium in the Bathing Solution

Experiment No.	Pup Age (days)	Transmembrane Potential (mV) initial	final	Comment
A. Response to low sodium Hank's BSS				
1	11	2.0	2.0	slow hyperpolarization to 3.0 mV, then rapid recovery
2	11	3.5	3.0	slight hyperpolarization, then slow depolarization
3	13	3.0	4.0	gradual slow hyperpolarization
B. Response to high potassium Hank's BSS				
1	11	2.5	2.5	slight hyperpolarization, then depolarization
2	11	4.0	3.0	Rapid depolarization
3	13	2.5	2.0	± 0.5 mV during solution change

low sodium and high potassium solutions (Table 3) were not distinguishable from the fluctuations of zero potential recorded during control solution changes, i.e., when no cell was impaled by the microelectrode during the solution change. The exchange of solutions in control experiments caused the baseline to shift by ± 0.5 mV.

Changing the bathing solution from standard to fluoride or calcium-free Hank's BSS (Table 4) caused more dramatic, but also more variable, responses of the transmembrane potentials. In three experiments, the change to fluoride Hank's BSS caused hyperpolarization of 0.5 mV, and 8.0 mV, or depolarization of 2.5 mV. In all three cases the transmembrane potential recovered to within 1.5 mV of the initial transmembrane potential.

In response to a change to calcium-free solutions two cells slowly hyperpolarized by 0.5 mV. One did not recover; the other depolarized slowly to 4.0 mV below its initial transmembrane potential. A third cell rapidly hyperpolarized by 11.0 mV, depolarized below, then recovered to, the initial transmembrane potential. A fourth cell responded by slowly depolarizing to 5.0 mV without recovery.

Control solution changes to fluoride or calcium-free Hank's BSS, without a cell impaled, showed variations of zero baseline potential of ± 0.5 mV. Thus, the magnitude of responses of transmembrane potentials to these solutions indicates a real, but highly variable, membrane response.

Table 4. Responses of Transmembrane Potentials of Osteoblasts to Changes of Fluoride and Calcium in the Bathing Solution

Experiment No.	Pup Age (days)	Transmembrane Potential (mV) initial	final	Comment
A. Response to fluoride Hank's BSS				
1	11	3.0	3.0	rapid hyperpolarization to 8.0 mV, and rapid recovery
2	11	3.5	2.0	depolarization to 1.0 mV, then recovery
3	13	4.5	3.0	slight hyperpolarization, then slow depolarization
B. Response to calcium-free Hank's BSS				
1	11	4.0	4.5	slow hyperpolarization
2	11	14.0	9.0	slow depolarization
3	13	4.0	4.0	rapid hyperpolarization to 15.0 mV, depolarization to 2.0 mV, then recovery
4	13	9.0	5.0	slight hyperpolarization, then slow depolarization

The transmembrane potential responses to a change to chloride-free Hank's BSS are shown in Table 5. In all experiments, the response to a change to chloride-free solution was that of hyperpolarization by 2.5 to 8.5 mV followed by slow depolarization to within 2.0 mV of the initial transmembrane potential. The response to a change from chloride-free to standard Hank's BSS was consistentently that of depolarization by 2.5 to 8.0 mV followed by slow hyperpolarization to within 4.0 mV of the initial transmembrane potential.

Control experiments, i.e., solution change without having a cell impaled, gave almost identical results to the cellular responses. In all 3 control experiments, however, the magnitude of response was more consistent. The control change from standard to chloride-free, and from chloride-free to standard caused peak responses of the magnitude of 6.0 to 7.0 mV. Figure 4 compares typical recordings of control (no-cell) and cellular responses. Obviously, the "cellular response" in this illustration cannot be considered anything other than a recording artifact (39) at the macroelectrode (reference electrode). Minimally, any real membrane response is masked by the magnitude of the artifact recording.

Results of experiments recording transmembrane potential responses to a change from standard to TCT Hank's BSS are given in Table 6. In all eight experiments there was an initial response of depolarization by 0.5 to 3.0 mV. In four experiments, the initial depolarization was followed by transient hyperpolarization of 1.5

Table 5. Responses of Transmembrane Potentials of Osteoblasts to Changes in Chloride Concentration of the Bathing Solution

Experiment No.	Pup Age (days)	Transmembrane Potentials (mV) initial	maximum	final	Comment
A. Change from Standard to Chloride-free Hank's BSS					
1	11	5.0	10.0	3.0	
2	12	7.0	15.5	5.5	
3	12	4.0	9.0	4.5	all hyperpolarized, then slowly depolarized to final value
4	13	4.0	6.5	3.0	
		6.0	10.5	6.5	
B. Change from Chloride-free to Standard Hank's BSS					
1	11	3.5	+0.5*	5.5	
2	12	5.0	0	4.0	
3	12	3.0	+5.0*	2.0	all depolarized, then slowly hyperpolarized to final value
4	13	5.0	1.5	9.0	
	13	7.0	4.5	7.0	

*(+) indicates reversal of polarity, e.g., recording below baseline zero

Figure 4. Typical Results of Chloride Solution Changes: Recordings of no-cell control and of cellular responses to changing the external solution from standard to chloride-free solution, and from chloride-free to standard solution are plotted against time.

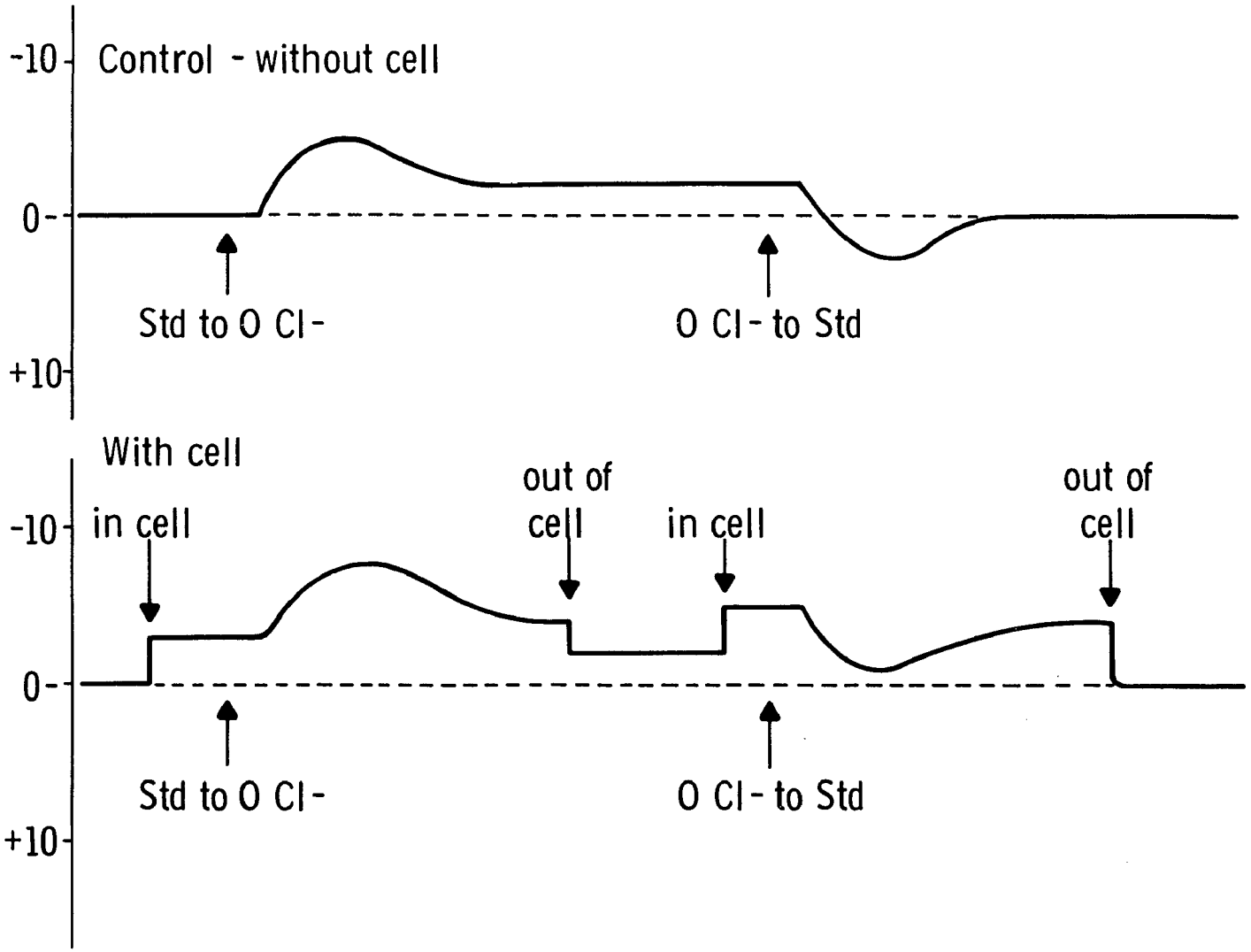
-10
Control - without cell
0
Std to O Cl-
O Cl- to Std
+10
With cell
-10
in cell
out of cell
in cell
out of cell
0
Std to O Cl-
O Cl- to Std
+10

Table 6. Responses of Transmembrane Potentials of Osteoblasts to a Change to TCT Hank's BSS

Experiment No.	Pup Age (days)	Transmembrane Potentials (mV)			
		initial	minimum[a]	maximum[b]	final[c]
1A	10	8.0	5.5	8.0	5.0
1B	10	7.5	4.5	16.5	14.5
2A	11	6.0	4.0	22.0	6.0
2B	11	4.0	3.5	5.5	2.5
3	12	8.5	8.0	8.5	8.0
4A	13	14.0	12.5	20.0	+2.5[d]
4B	13	5.5	2.5	2.5	2.5
5	14	3.0	2.5	3.5	1.0

[a] minimum transmembrane potential observed during change of solution.

[b] maximum transmembrane potential observed within 20 minutes after completion of change of solution.

[c] final transmembrane potential usually taken within 30 minutes after completion of change of solution.

[d] (+) indicates reversal of polarity.

to 16.0 mV above the initial transmembrane potential. In three experiments, the membrane recovered from the initial depolarization to within 0.5 mV of the initial transmembrane potential. The other one experiment resulted in slow continuous depolarization without recovery.

The final transmembrane potentials were taken between 13 and 30 minutes after completion of the change of solution, except for one experiment (No. 4A) which was extended to 75 minutes to see if the cell would recover from the reversal of polarity which had occurred at 30 minutes. As noted by the final transmembrane potential recorded for this experiment (Table 6), the cell did not recover.

In two of those experiments in which hyperpolarization was recorded (Nos. 1B and 4A), a rise in tip resistance occurred simultaneous with the hyperpolarization. This could indicate a microelectrode artifact rather than actual hyperpolarization of the cell. However, in experiment No. 2A, which showed the greatest hyperpolarization, no change in tip resistance occurred.

The results of the in vivo experiments are given in Table 7. A total of 16 recordings of transmembrane potentials from three 10- or 11-day old pups were made. The mean transmembrane potential recorded in vivo was 1.72, with a standard error of ± 1.07. The number of experiments is small and, of itself, this series of experiments is inconclusive. However, these results do give an "order of

Table 7. *In Vivo* Transmembrane Potentials of Osteoblasts

Pup No.*	1	2	3
	2.0	3.0	1.0
	0.5	1.5	1.5
	1.0		1.5
	0.5		1.0
	4.0		3.5
	2.5		
	1.5		
	1.5		
	1.0		
Overall Mean	1.72		
Standard Error	±1.07		

* All 3 pups were 10 or 11 day old littermates.

magnitude" verification of the mean transmembrane potential recorded *in vitro*.

Discussion

The recorded transmembrane potentials of osteoblasts, both *in vivo* and *in vitro*, are low, but correspond in magnitude to those recorded for osteoclasts.

The lack of response of these cells to changes in sodium or in potassium concentrations in the bathing solution indicates that the osteoblast membrane is impermeable to both ions, or that their relative permeabilities are near unity. Either postulate is possible. Also, cellular damage upon penetration of the cell by the microelectrode could cause these same results.

Before considering the case of impermeability to both ions we should consider those in which the membrane is permeable to sodium, to potassium, or to both. In a cell whose measured transmembrane potential is 4 mV, inside negative, and whose membrane is selectively permeable to potassium, the Nernst equation,

$$V = \frac{-RT}{zF} \ln \frac{C \text{ in}}{C \text{ out}}$$

predicts that the intracellular potassium concentration is 6.72 mM with a concentration of 5.74 in the external solution. By the same method, this same cell, selectively permeable to sodium, would have an intracellular sodium concentration of 165.81 mM with a concentration of 141.72 in the external solution.

If the membrane were selectively permeable to both sodium and potassium with a permeability ratio of 1.0, the Goldman equation,

$$V = \frac{-RT}{zF} \ln \frac{C_1 \text{ in} + C_2 \text{ in}}{C_1 \text{ out} + C_2 \text{ out}}$$

predicts a combined intracellular concentration of sodium and potassium of 171.36 mM. With equal permeabilities the ratios of distribution of ions across the membrane would have to be equal. Thus the major part of this 171.36 mM would have to be sodium.

Now consider the case for impermeability of the membrane to both ions. In this case, both ions could be distributed unequally across the membrane with only the permeant anions being guided by (or guiding) the transmembrane potential.

The erythrocyte membrane is a known example of a membrane impermeable to both sodium and potassium. It also has a low transmembrane potential of 11 mV, inside negative. Flux studies have shown an apparent (but not absolute) impermeability to both ions, with active accumulation of potassium and extrusion of sodium. The transmembrane potential is a Gibbs-Donnan potential imposed on the permeant anions by the nondiffusable anionic hemoglobin (13).

It is noteworthy that the osteoblasts and erythrocytes have origin from the same mesenchymal cells of bone marrow. Thus, it is not unlikely that they would have similar membrane characteristics. However, as discussed, the membrane may be equally permeable to both sodium and potassium.

Also, cellular damage at the site of entry of the microelectrode could serve as a large "leakage" pathway for all ions.

In this case, the recorded transmembrane potential, as well as responses to all ionic changes in the external solution, would be erroneous. However, the possibility exists that the potential of osteoblasts is determined by some other, as yet unidentified ion.

Before leaving the discussion of potassium and osteoblast membranes, comments on recent papers (10, 16, 45) aimed at establishing evidence for a "bone membrane" are indicated. These studies, showing a high potassium content of bone as the major evidence, were done on cortical bone supposedly devoid of cellular material. Yet the one study in which any indicator of cellular content was measured reported DNA and hemoglobin in concentrations of 1.3 mg/g and 0.12 mg/g, respectively (16). This certainly indicates a high proportion of cellular material was present. In fact, in a separate study (34) of bone diaphyses from which the marrow was not removed, a DNA content of only 0.0069 μg/mg was reported. Even allowing 200% error in these values, a large cellular element must have been present in the samples for both studies. The possibility of a cellular origin of the potassium cannot be excluded.

In the same study of potassium in bone (16) a metabolic inhibitor (iodoacetate) caused the release of large amounts of potassium from intact calvaria, supposedly from a separate bone extracellular fluid. I propose that the inhibitor acted to release intracellular potassium.

The responses of the membrane potential to fluoride and to calcium-free solutions can be explained on the basis of an assumed

impermeability or equal permeability of the membrane to sodium and potassium. Again, the model of the erythrocyte membrane will be used (13). In these cells, fluoride causes an increased permeability to potassium only. Decreased external calcium concentrations cause an increased permeability to both sodium and potassium. However, fluoride in a calcium-free solution has no effect on membrane permeabilities. The exact mechanisms involved in these phenomena are unknown but they are thought to be related to the regulation of the calcium "pump".

With increased permeability to potassium, hyperpolarization is expected. Fluoride solutions caused hyperpolarization in 2 of 3 experiments on osteoblasts.

With increased permeability to sodium and potassium, hyper- or depolarization could occur depending on the relative increases of permeabilities to the two ions. In experiments on osteoblasts, calcium-free solutions caused hyperpolarization in 3 of 4 experiments and depolarization in the other one. Thus, the variable responses of osteoblasts may reflect differences in the ratio of permeabilities induced. Also, since both fluoride and calcium-free solutions are thought to exert this effect through the calcium "pump", the variable response of the osteoblasts may depend on the status of the cell's calcium "pump" at the time of the experiment.

The effects of TCT on the transmembrane potentials were much more dramatic, causing large magnitude hyperpolarizations in four of eight experiments. These results agree well with those reported

for osteoclasts, where an average hyperpolarization of 12.6 mV was found (29).

Hyperpolarization would occur with an increase in membrane permeability to potassium or phosphate, assuming concentration gradients directed outward for potassium and inward for phosphate.

Borle has reported that TCT inhibits the active efflux, without affecting the passive influx, of calcium from the cytoplasm to the extracellular fluid (8). Reasonably, the accumulation of calcium ions intracellularly could affect phosphate or potassium permeability to cause the hyperpolarization. Also, the influx of calcium which tends to depolarize the membrane could be retarded by the cytoplasmic accumulations of calcium caused by the inhibition of calcium efflux. This would result in hyperpolarization.

Borle also reported in the same study that the effects of TCT were transient, with a maximal inhibition of efflux occurring within 30 minutes. The time course of the transmembrane responses of osteoblasts to TCT confirm the transient character of the TCT effects.

CHAPTER 3

DYE INJECTION INTO OSTEOBLASTS

Historically, the marking of areas from which potentials were recorded was developed to facilitate studies of the central nervous system (1). These marks were made by passing current through a metal wire to deposit ions of silver or iron which could later be stained in tissue sections.

After the development of glass microelectrodes, these same techniques of depositing ions of heavy metals in the tissue were used by filling the microelectrodes with solutions of these ions (32). These techniques were refined to give immediate localization without sectioning the tissue, by depositing ferrocyanide ions from the potassium ferrocyanide filled microelectrodes, then immediately adding ferric chloride to the bathing solution to develop the Turnbull's blue mark (44).

At about this same time (Ca, 1960) methods were developed to fill glass microelectrodes with charged dye molecules which could be directly electrophoresed into the tissue. The lithium carmine filled microelectrodes which are used in this study were used by Villegas (46) in studies of the gastric mucosa.

In 1964, Loewenstein and Kanno used dye injection (by pressure, not electrophoresis) of sodium fluorescein to confirm their finding of cell-to-cell communications (26). These cells had previously been shown to have communications capable of conducting electrical impulses (21).

The injection of dye into osteoblasts in these experiments was used to establish the functional capacity of the anatomical communication (tight junctions) which had been demonstrated between osteoblasts (18, 48).

Methods and Procedures

Twenty female albino rats with litters of 8 to 10 pups each were obtained for use in dye injection experiments. One to six pups of each litter were used; one to five experiments were performed on each pup. A total of 210 experiments were performed on eighty different 7- to 20-day old pups.

The techniques of tissue preparation, the chamber, and the microscopic and manipulator set-ups were the same in these experiments as that used for the _in vitro_ transmembrane potential experiments (Chapter 2).

The microelectrodes were cleaned and pulled as for recording microelectrodes, but were filled directly with a lithium carminate dye solution by boiling under vacuum. The dye solution was initially prepared as a 1% solution (w/v) in 3 M KCl. It was then filtered

twice through a sintered glass filter with plain paper filters with pore sizes of 0.8, then 0.4, micron. Thus, the final dye concentration was somewhat less than 1%.

Carmine dyes are natural dyes prepared from the echinoderm of insects. The lithium carminate preparation was obtained from Matheson, Coleman, and Bell*, who reported that this dye has not been processed since 1952. The exact procedure for its preparation has been lost from the records of this company. Thus, the dye is an old, natural dye of unknown composition. However, assuming it is similar to other carmine dyes, it has an approximate molecular weight of 500 (24) and carries a variable negative charge.

The dye-filled microelectrodes had tip potentials of 50 to >100 mV and tip resistances of >100 MΩ. Microelectrodes with such high tip resistances do not have stable recording properties. The observed transmembrane potential was used only as confirmation of cell impalement. Consequently, no attempt was made to correlate dye injection with any electrical parameters of the cells.

The electrical arrangement for dye injection experiments is illustrated in figure 5. The dye-filled microelectrode was connected by a silver-silver chloride wire to a switch box so that it could be connected to either the amplifier-recorder or the current source-recorder circuit. A second silver-silver chloride wire from the bathing solution to ground completed both circuits.

---

*Matheson, Coleman, and Bell, Division of the Matheson Company, Inc., Norwood (Cincinatti), Ohio.

Figure 5. Dye Injection Electrical Set-Up: A dye-filled micro-electrode is connected by a silver-silver chloride wire to a switch box so that it can be connected to either an amplifier and recorder or to a current source and recorder (across a 5 MΩ resistance). A second silver-silver chloride wire from the bathing solution through the switch box to ground on the amplifier, current source and both recorders completes both circuits.

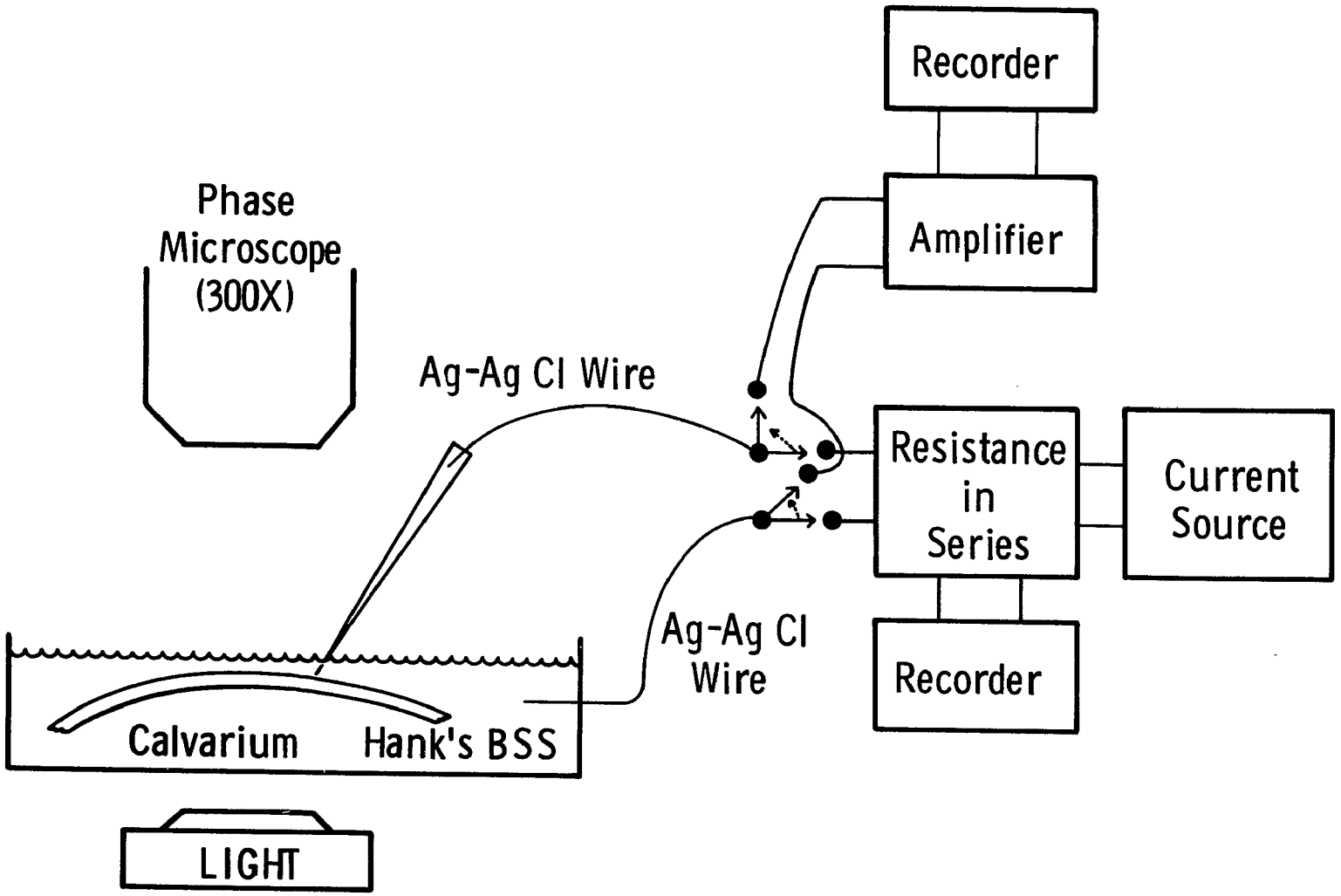
Recorder
Amplifier
Phase
Microscope
(300X)
Ag-Ag Cl Wire
Resistance
in
Series
Current
Source
Ag-Ag Cl
Wire
Recorder
Calvarium
Hank's BSS
LIGHT

The current source was a battery-ammeter which allowed variation of the voltage imposed from 45 to 135 volts with continuous monitoring of the current in the circuit. The current source also had internal switches to further isolate (besides the switch box) the two circuits and to reverse the polarity of the imposed voltage.

Besides the ammeter monitor of the current in the circuit, the current passing through the microelectrode was measured by recording on a mV recorder the potential drop across a 5 MΩ resistance arranged in series with the microelectrode. The current could then be calculated by Ohm's law ($I = \frac{V}{R}$). The calculated current generally agreed with the ammeter reading. However, the calculated current was more accurate since the mV recorder damped the overshoot induced by the instantaneous reversal of polarity better than did the ammeter.

With the microelectrode connected to the amplifier-recorder, an osteoblast was impaled. Then the microelectrode was switched to the current source-recorder circuit for electrophoretic injection of the dye into the impaled cell. Positive current was passed into the microelectrode for 5 to 30 seconds, then the polarity reversed for 1 or 2 seconds. Reversal of the current was accompanied by an immediate release of a small amount of dye into the cell.

Experiments were recorded photographically. Some 35 mm still and some 8 mm movies were taken. Location of the injected dye was confirmed histologically in frozen and in paraffin-embedded sections. The sections were stained with either colloidal iron or toluidine

blue stain. To minimize dissolution and dislocation of the water soluble lithium carmine dye, the staining procedures were modified to use alcoholic solutions. The exact protocol for the histologic procedures is given in detail in Appendix 2.

Results

During dye injection into any one cell, the dye rapidly moved into nearby cells, often into more than twenty cells. These observations were recorded photographically. Although the cells were impaled and injected under phase microscope visualization, the photographs were made without the phase annulus. The annulus reduces light transmission to such a degree that the pictures of the calvaria with it in place were too dark.

Plates 1 and 2 are 35 mm photographs taken through the microscope during an experiment. In plate 1 (A) the microelectrode is in a cell before the beginning of dye injection. Plate 1 (B) shows the same cell, into which the dye has now been injected. Other surrounding cells also contain the dye. The area surrounding the microelectrode looks very dark and undetailed because of the overlapping of the images of successive layers of cells. The details of individual cells in such an area are better seen in cross section (Plates 5, 6, and 7). Plate 2 (A) shows the further movement of dye with continued injection into the same cell. More cells, both superficially and deeply located within the tissue, now

Plate 1. Dye Injection: (A) Microelectrode is in a cell just prior to beginning dye injection, (B) Beginning of dye injection into the same cell as in (A). ~ 100x.

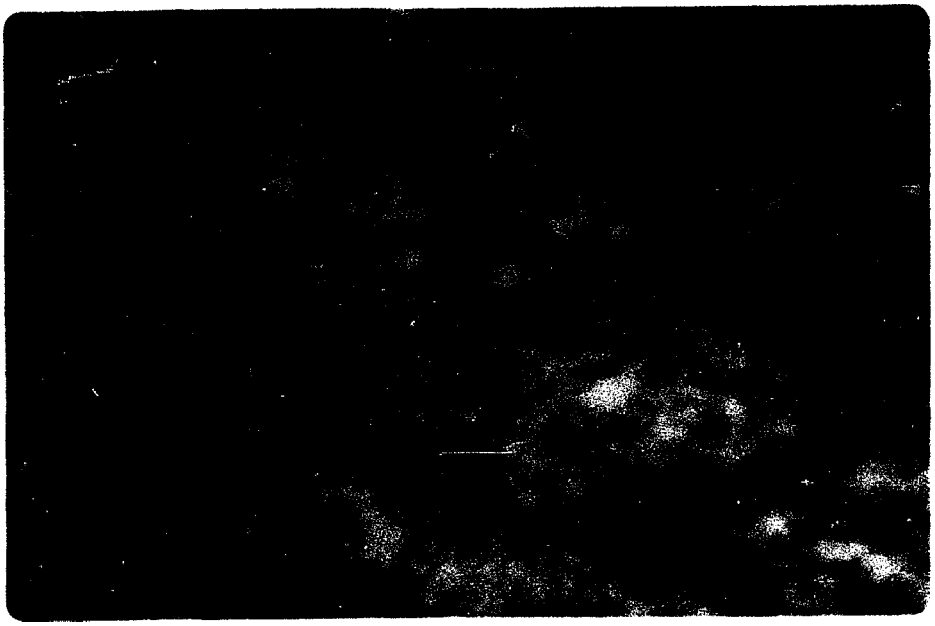

Plate 2. Dye Injection: (A) Continued dye injection into the same cell as in Plate 1, (B) Completed dye injection with the microelectrode removed. ~ 100x.

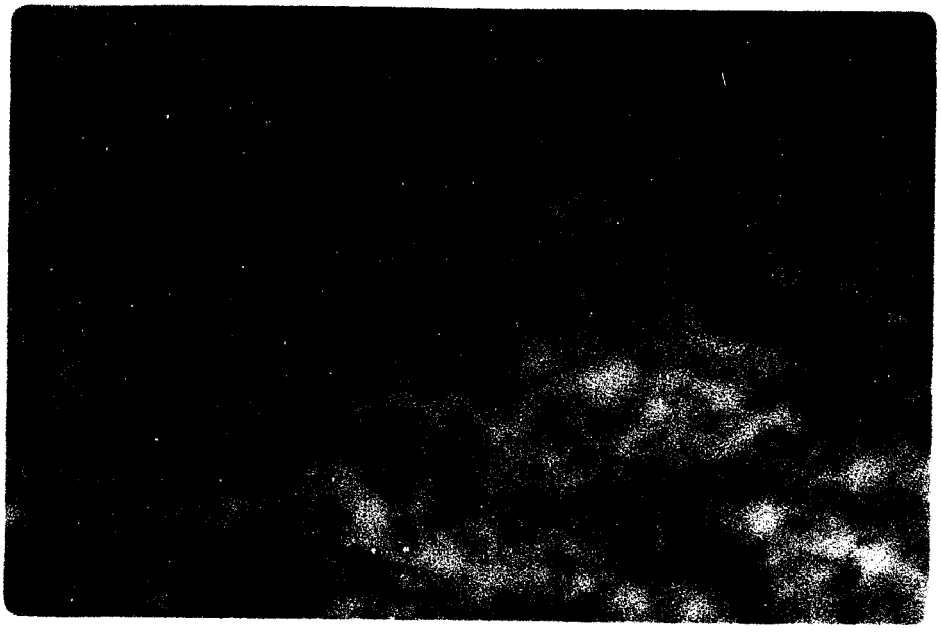

contain the dye. Plate 2 (B) shows the same area after completion of the experiment and removal of the microelectrode. More than twenty-five cells contain the dye injected into only one cell. The cells containing the dye have a latticework arrangement. With the phase annulus the areas within the lattice have many cells which do not contain the dye.

The movement of the dye with each current pulse was very rapid. To demonstrate the dynamics of the dye injection process, 8 mm movies were taken through the microscope in some experiments. Plates 3 and 4 are prints made from one 16-frame sequence of one current pulse from the middle of one experiment. Plate 3 (A) corresponds to the time just after the reversal of polarity and the beginning of a pulse of dye. Plates 3 (B) and 4 (A) and (B) are every fifth frame thereafter. Thus, all four prints represent in time less than 0.9 second. Plate 3 (B) shows dye movement beginning to the right and above the microelectrode. Plate 4 (A) shows continued dye movement above the microelectrode. Plate 4 (B) shows the extent of dye movement with this single current pulse.

The dye moved more than 30 microns in less than 0.9 second. Thus, the calculated velocity of the dye is 3.33×10^{-3} cm/sec.

This series of pictures also shows very well the often-encountered movement of the dye in specific directions, rather than equal movement in all directions.

Plates 5, 6, and 7 are photomicrographs of cross sections of tissue from areas of dye injection. Plates 5 (A) and (B) are

Plate 3. A Single Pulse of Dye, recorded by an 8 mm movie camera: (A) Just after reversal of polarity, (B) 5 frames (< 0.3 second) later than in (A). ~ 100 x.

Plate 4. A Single Pulse of Dye, recorded by an 8 mm movie camera: (A) 5 frames (< 0.3 second) later than in Plate 3 (B), (B) 5 frames (< 0.3 second) later than in (A). ~ 100x.

pictures of two frozen sections. In plate 5 (A), the tissue has been stained with toluidine blue. Cellular membranes are well-stained, so the intracellular location of the dye is clearly demonstrated in this picture. The tissue in plate 5 (B) has been stained with colloidal iron. It is a pale yellow stain here, probably due to the alcoholic solutions used for staining (see Appendix 2' for details). The close relationship of a few dye-containing cells and the bone matrix is obvious in this picture.

Plates 6 and 7 are photomicrographs of paraffin sections stained with colloidal iron. Collectively, these pictures demonstrate the variety of numbers and of relationships of the dye-containing cells, one to another and to the underlying bone matrix.

The currents used for dye injection were recorded in eleven experiments. The range was 2.9 to 6.8 x 10^{-6} amp, with a mean of 5.1 x 10^{-6} amp.

Discussion

The observed movement of dye between osteoblast cells confirms the physiologic significance of the tight junctions reported to occur between osteoblasts and with osteocytes (18, 48). However, the time required for dye movement in these cells is much faster than that observed in salivary glands (26) or axons (22). Most likely the use of electrophoresis rather than hydrostatic pressure to inject the dye into the cells is responsible for the rapid dye migration. However,

Plate 5. Frozen Cross Sections of Calvaria, taken from an area of dye injection: (A) Counterstained with toluidine blue, (B) Counterstained with colloidal iron. ~ 100x.

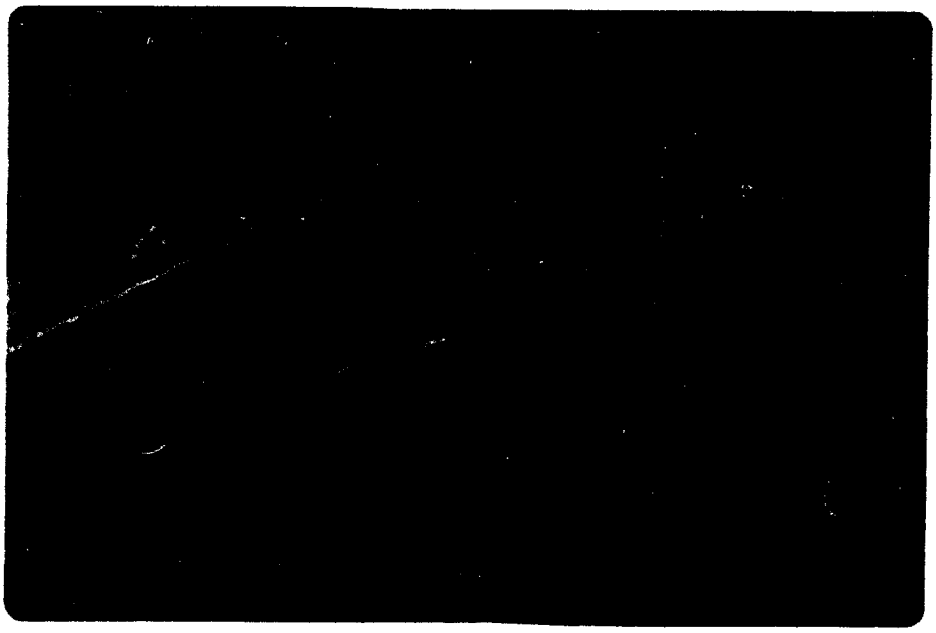

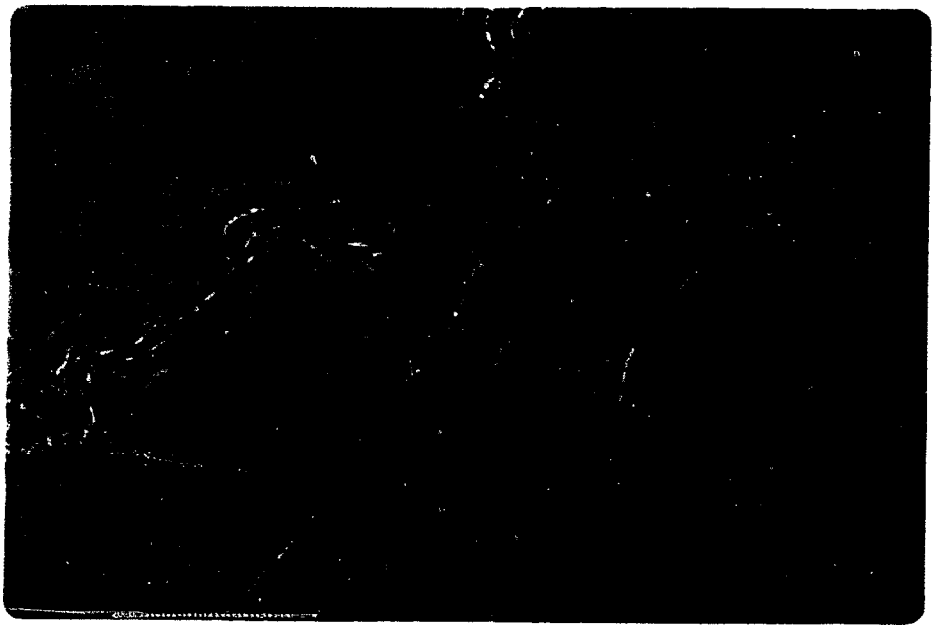

Plate 6. (A) and (B). Paraffin Cross Sections of Calvaria, taken from an area of dye injection and counter-stained with colloidal iron. ~100x.

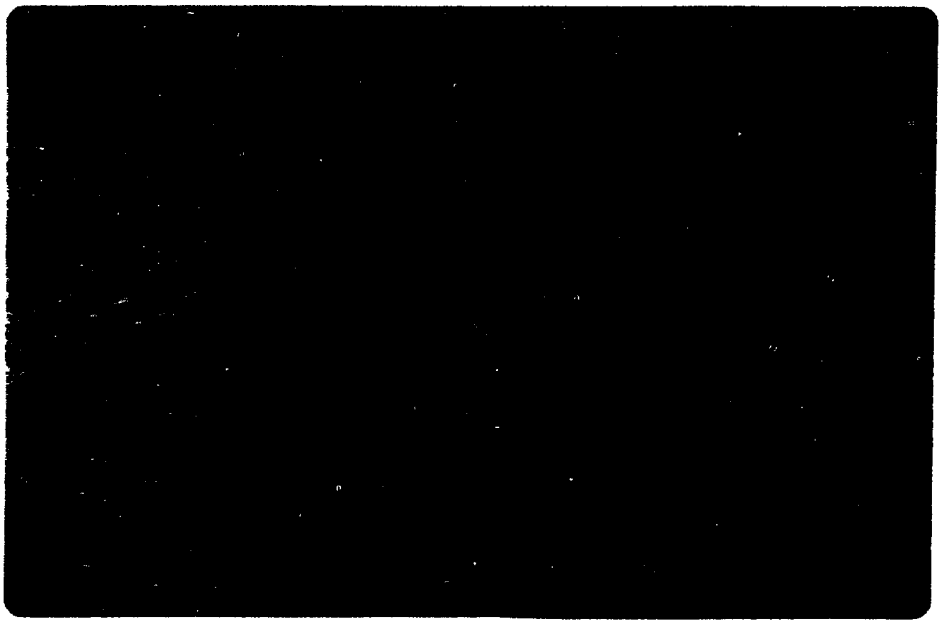

Plate 7. (A) and (B). Paraffin Cross Sections of Calvaria, taken from an area of dye injection and counter-stained with colloidal iron. ~100x.

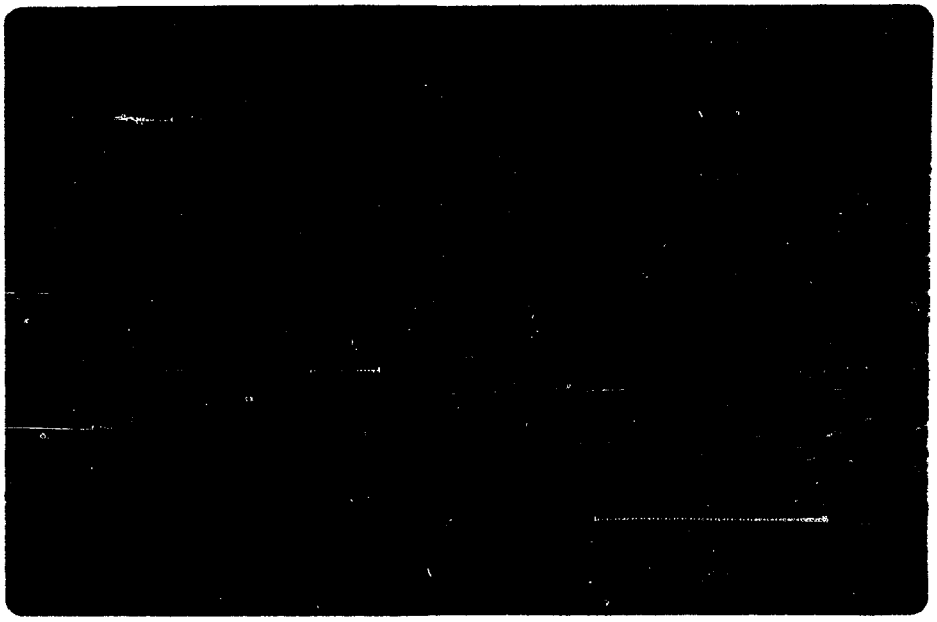

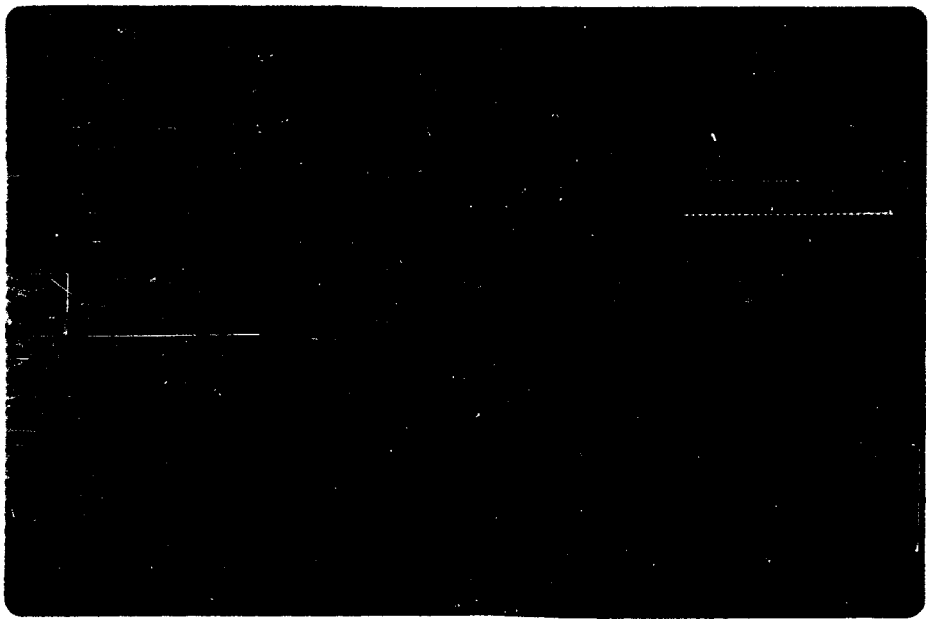

the microtubular systems and microfilaments of osteoblast and osteocyte processes have been proposed to serve in fluid movements within these cells (18). The results reported here do not unquestionably affirm this proposal but they do emphasize the possibility of such fluid movements. Certainly, they could account for the rapid responses of osteocytes to hormones.

CHAPTER 4

ELECTRICAL COUPLING OF OSTEOBLASTS

Numerous studies of the permeabilities of intercellular communications have been performed on many tissues since the techniques were first introduced in 1964. Some of these cell junctions are permeable to ionic current, but impermeable to large molecules such as dyes. In fact, there is mounting evidence that morphologically specific types of cell junctions are concerned with specific functions, e.g. gap junctions are associated with electrical coupling (3).

Thus, it is necessary to the further characterization of the intercellular communications of osteoblasts to determine their ionic (electrical) permeability characteristics, as well as their permeability to larger molecules (dyes).

Studies of the electrical properties of cell junctions were first performed using three microelectrodes, two in one cell and one in another cell (21). With this arrangement current is sent through one cell and the resulting changes in transmembrane potentials of both cells can be recorded. Mathematical analysis of voltage versus distance by the cable theory allows determination of the surface resistance and of the cytoplasmic resistance.

A recent paper (15) describes a technique for obtaining these same measurements using two microelectrodes with a different mathematical analysis. This technique is most applicable to small cells, such as osteoblasts, where it is difficult, if not impossible, to put two microelectrodes in one cell. This technique was used in the present experiments.

Methods and Procedures

Three female albino rats with litters of 8 to 10 pups each were obtained for use in experiments to measure the extent of electrical coupling between osteoblasts. Eighteen experiments were performed on eleven of these pups in the age range of 6- to 24-days old.

The techniques of tissue and microelectrode preparation, the chamber, and the microscopic and manipulative set-up was the same in these experiments as that used for *in vitro* transmembrane potential recordings (see Chapter 2). The experimental set-up is illustrated in figure 6. Two microelectrodes were used with separate micromanipulators and electrical circuits. One microelectrode (the recording microelectrode) was connected by a 3 M KCl agar bridge and calomel electrode to an amplifier-recorder. A second 3 M KCl agar bridge and calomel electrode from the bathing solution to ground on the amplifier and recorder completed the circuit. The second microelectrode (the current microelectrode) was connected by

Figure 6. Electrical Set-Up to Measure Osteoblast Coupling: Two microelectrodes are used in separate electrical circuits. One microelectrode is connected by a silver-silver chloride wire to a switch box so that it can be connected to either an amplifier and recorder or to a current source and recorder (across a 5 MΩ resistance). A second silver-silver chloride wire from the bathing solution through the switch box to ground on the amplifier, current source and both recorders completes both circuits. The second microelectrode is connected by a 3 M KCl agar bridge and calomel electrode to a high impedance amplifier and mV recorder. This circuit is completed by a second 3 M KCl agar bridge and calomel electrode from the solution in the chamber to ground on the amplifier and recorder.

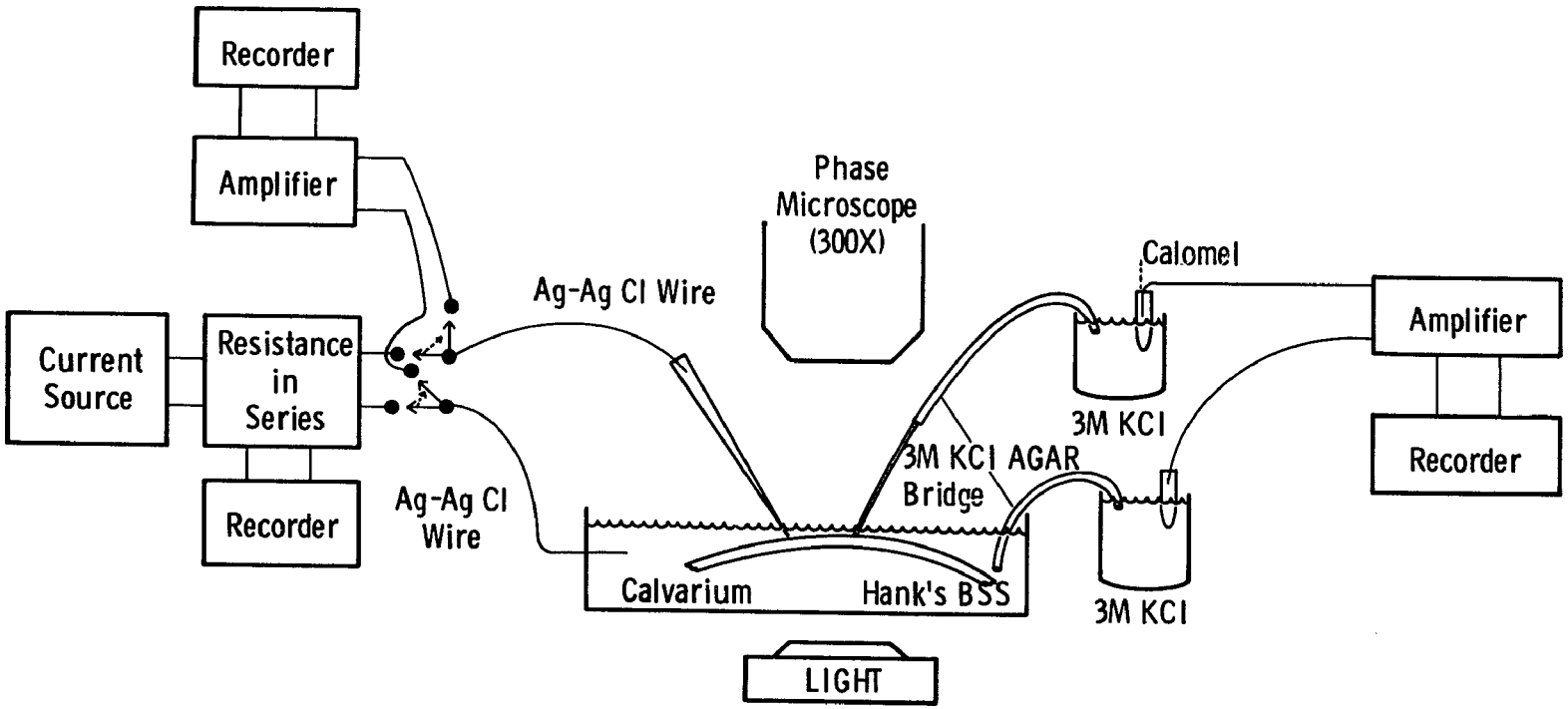
Recorder
Amplifier
Phase
Microscope
(300X)
Calomel
Ag-Ag Cl Wire
Amplifier
Current
Source
Resistance
in
Series
3M KCl
3M KCl AGAR
Bridge
Recorder
Recorder
Ag-Ag Cl
Wire
Calvarium
Hank's BSS
3M KCl
LIGHT

a silver-silver chloride wire to a switch box. This switch allowed the microelectrode to be connected to a separate amplifier-recorder circuit or to a current source-recorder circuit. A second silver-silver chloride wire from the bathing solution was connected through the switch box to ground on the amplifier, the current source and both recorders.

In each experiment, separate cells were impaled by both microelectrodes simultaneously. The distance between the two cells was measured with a micrometer eyepiece on the microscope and recorded. When both transmembrane potentials had been stable for at least 30 seconds, the current microelectrode was switched to the current source circuit. A pulse of current was sent for approximately 2 seconds through the microelectrode. The current sent was measured as the voltage drop across a 5 MΩ resistance in series with the microelectrode.

The response of the transmembrane potential of the cell impaled by the recording microelectrode was simultaneously recorded. Then, the recording microelectrode only was removed from the cell. A new cell, at a different distance from the cell impaled by the current microelectrode, was impaled. Both transmembrane potentials were checked for stability, and the new distance between cells was recorded. Then the same current was again sent through the current microelectrode and measured. The response of the transmembrane potential of the new cell was simultaneously recorded.

In each experiment responses of at least four different cells at different distances from the cell containing the current microelectrode were recorded. At the conclusion of some experiments the recording microelectrode was placed in contact with the tissue but not within a cell. The same current was passed through the current microelectrode, and the response of the recording microelectrode to current reaching it through extracellular tissue connections was recorded.

The data from each experiment were subjected to mathematical analysis for the current spread in the tissue (15). The analysis used is a computerized program based on a Bessel function solution of the cable theory of the spread of current in a thin sheet. Details of the mathematical analysis are given in Appendix 3. Briefly, the analysis gives a solution of the current spread in terms of two parameters,

$$A = \frac{I_o R_i}{2\pi L} \quad \text{and} \quad \lambda = \sqrt{\frac{L R_z}{R_i}}$$

where: I_o is the injected current; R_i is the internal resistance of the tissue for current flow within the plane, given in Ω cm; R_z is the resistance for current flow perpendicular to the plane, i.e., leaving the tissue, given in Ω cm^2; and L is the tissue thickness. From these two parameters $R_{i/L}$ (Ω) and R_z (Ω cm^2) can also be evaluated as,

$$R_z = \frac{2\pi A\lambda^2}{I_o}$$

and

$$\frac{R_i}{L} = \frac{2\pi A}{I_o}$$

Results

The passage of current between an intracellular microelectrode and an electrode in the bathing solution resulted in voltage changes in the transmembrane potentials of cells impaled by a second microelectrode. Transmembrane potential changes as high as 10.6 mV and as low as 0.1 mV were recorded in response to currents of 20 to 60 x 10^{-8} amp.

The results of one experiment are illustrated in figure 7. In this experiment, as in most other experiments, the transmembrane potential response was greatest at the smallest distance between the two cells and least at the greatest distance. The open circles are actual experimental values recorded in response to a current of 40×10^{-8} amp. The solid curve is the zero-order modified Bessel function, fitted with the parameters A = 0.779 mV and λ = 290.2 microns.

The Bessel function solution of cable analysis of the spread of current yielded fairly consistent results for the parameters A and λ and for the calculated values $R_{i/L}$ and R_z. These values for each experiment are recorded in Table 8. The mean values were A = 0.781 mV, λ = 320.2 microns, $R_{i/L}$ = 15.2 KΩ, and R_z = 11.95 Ω cm^2.

Figure 7. Electrical Coupling between Osteoblasts: Results of a Typical Experiment. The changes of the transmembrane potentials of cells at various distances from a cell into which 40 x 10^{-8} amp is injected are plotted as open circles. Distances in microns are the abscissa; resultant changes in transmembrane potential in mV are the ordinate. The solid curve is the Bessel Function Solution.

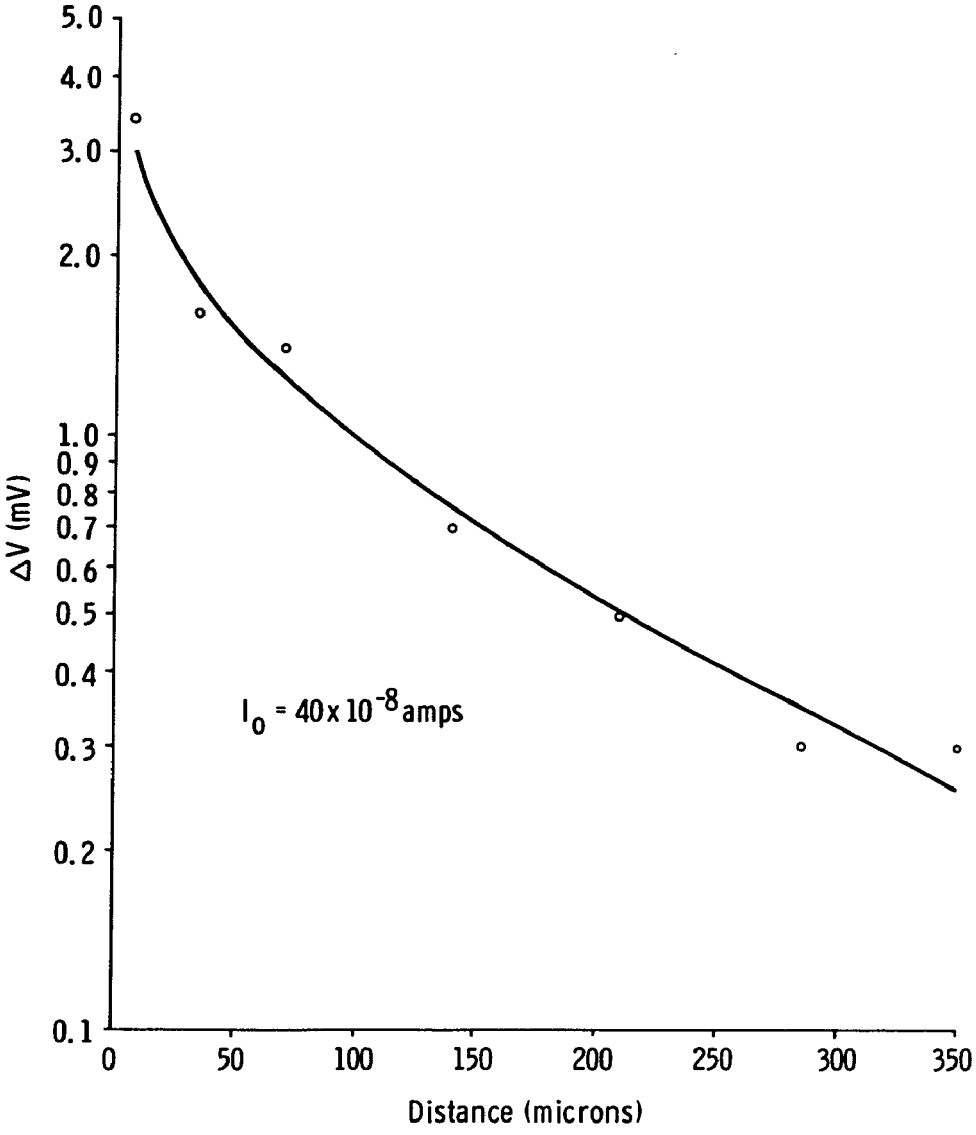
5.0
4.0
3.0
2.0
1.0
0.9
0.8
0.7
0.6
0.5
0.4
0.3
0.2
0.1
ΔV (mV)
$I_0 = 40 \times 10^{-8}$ amps
0
50
100
150
200
250
300
350
Distance (microns)

Table 8. Bessel Function Analysis of Current Spread in Osteoblasts

Experiment No.	Pup Age (days)	I_o ($\times 10^{-8}$ amps)	A (mV)	λ (microns)	R_i/L (KΩ)	R_z (Ω-cm^2)
1	6	60	0.613	262.2	6.42	4.42
2	9	28	0.320	511.9	7.17	18.79
		44	0.472	498.5	6.73	16.73
		50	0.577	444.5	7.25	14.33
3	9	20	0.364	374.2	11.44	16.01
4	13	30	3.159	92.0	66.16	5.60
5	13	40	1.588	147.7	24.94	5.44
6	16	30	0.662	258.3	13.86	9.25
		40	0.779	290.2	12.55	10.57
7	16	20	0.342	351.4	10.75	13.27
		30	0.386	577.9	8.08	27.00
		40	0.438	708.0	6.87	34.45
8	20	30	0.596	197.1	12.48	4.85
		40	0.862	183.1	13.54	4.54
9	20	30	0.572	284.0	11.99	9.67
10	24	22	0.696	179.1	19.88	6.38
		30	0.908	176.9	19.02	5.95
11	24	30	0.728	225.8	15.24	7.78
Mean			0.781	320.2	15.24	11.95
±S.D.			±0.662	±167.9	±13.69	±8.30

Discussion

The results of the electrical coupling experiments confirm the postulate that the cell junctions of osteoblasts can transmit ionic current and thus may possibly serve as pathways for calcium and hormone movements between cells. This statement must be made with caution in view of the results of experiments (27) in which ionic calcium was injected into a cell having junctions with other cells. The intracellularly injected calcium caused rapid (< 2 minutes) uncoupling of the cells.

In view of the known effect of both calcium-regulating hormones to increase the cytoplasmic concentrations of calcium, it would be interesting to determine the response of osteoblast coupling to these hormones.

In experiments where the transmembrane potentials of cells were measured during uncoupling, they declined (depolarization) with uncoupling (33). The depolarization was related to uncoupling, since the uncoupling could be prevented by passing polarizing currents through the cell. In the experiments studying TCT effects on transmembrane potentials (Chapter 2), they sometimes increased (hyperpolarization). Thus it is possible that the high intracellular calcium induced in these cells by TCT by the inhibition of efflux from cytoplasm to the extracellular fluid does not uncouple osteoblasts.

The inward movement of calcium would depolarize the cell, thus some other electrogenic mechanism must hyperpolarize the cell. As

mentioned previously (Discussion, Chapter 2), this hyperpolarization may result from a transient increase in potassium permeability.

Assuming a high intracellular calcium has the potential to uncouple cells and in the light of the necessity of bone cells to maintain cell junctions for calcium movement, this transient hyperpolarization serves a very significant function in osteogenic cells.

The magnitude of response and the calculated values for λ, $R_{i/L}$, and R_z are within the range of those reported for other tissues (28).

The value of $R_{i/L}$ reported for osteoblasts may be converted to R_i by multiplying by the cell thickness, 10 microns. This gives an average value of R_i for osteoblasts of 15.2 Ω-cm. If the allowance for cell geometry differences is made, i.e. the processes of osteoblasts and small areas of cell membrane fusion make the only contacts for current flow so the effective tissue thickness is at least less than 1 micron, the calculated R_i is 152 Ω-cm. This compares well with values of 140-150 and 180 reported for salivary gland and toad bladder, respectively (28).

Similar comparisons of the values of R_z were made: osteoblast, 11.95 Ω cm^2; salivary gland, 9,000; urinary bladder, $\leq$100. The resistance of the surface membrane of osteoblast may be interpreted as very low from these comparisons. However, comparison of λ for the three tissues shows: osteoblasts, 320.2 microns, salivary gland, 750-1100; toad bladder, 18. The value for osteoblasts is

intermediate, but again is an underestimate because of the geometry of bone cells.

The interpretation of these results collectively shows that bone cells are, as a minimal estimate, at least as coupled as toad bladder cells, and possibly as highly coupled as salivary glands if allowance is made for osteogenic cell geometry.

CHAPTER 5

INTACT CALVARIUM AS A MEMBRANE

In the study of bone potassium in rat calvaria cited previously (16) it was reported that merely scraping the surface resulted in disruption of the bone "membrane" and subsequent release of large amounts of potassium from the proposed "separate bone extracellular fluid". This suggested to me that the entire periosteum of the calvarium was the membrane. The following study was designed to test the membrane properties of the rat calvaria in a system used to study many membranous tissues.

Methods and Procedures

Experiments to measure the transtissue potential and resistance of bone were performed on the calvaria of rat pups. Eight 9- to 12-day old albino rat pups from a single litter were used. The calvarium was excised and the surface facing the brain in the intact animal was carefully scraped to remove the surface osteoblasts. The tissue was placed between two chambers (38) of small (0.36 cm^2) active area (12). The chambers and the location of the tissue between them are diagramed in figure 8.

Figure 8. Chambers and Electrical Set-Up Used to Test the Membrane Properties of Whole Calvaria: Each chamber contains two electrodes, a lead-lead acetate agar electrode for sending current and a calomel electrode for recording potentials. The tissue is placed between the two chambers, and the chambers clamped together. Both chambers are filled with standard Hank's BSS, then the solution on the skin side of the calvarium changed to the experimental solution. The potential difference between the calomel electrodes is recorded on a mV recorder.

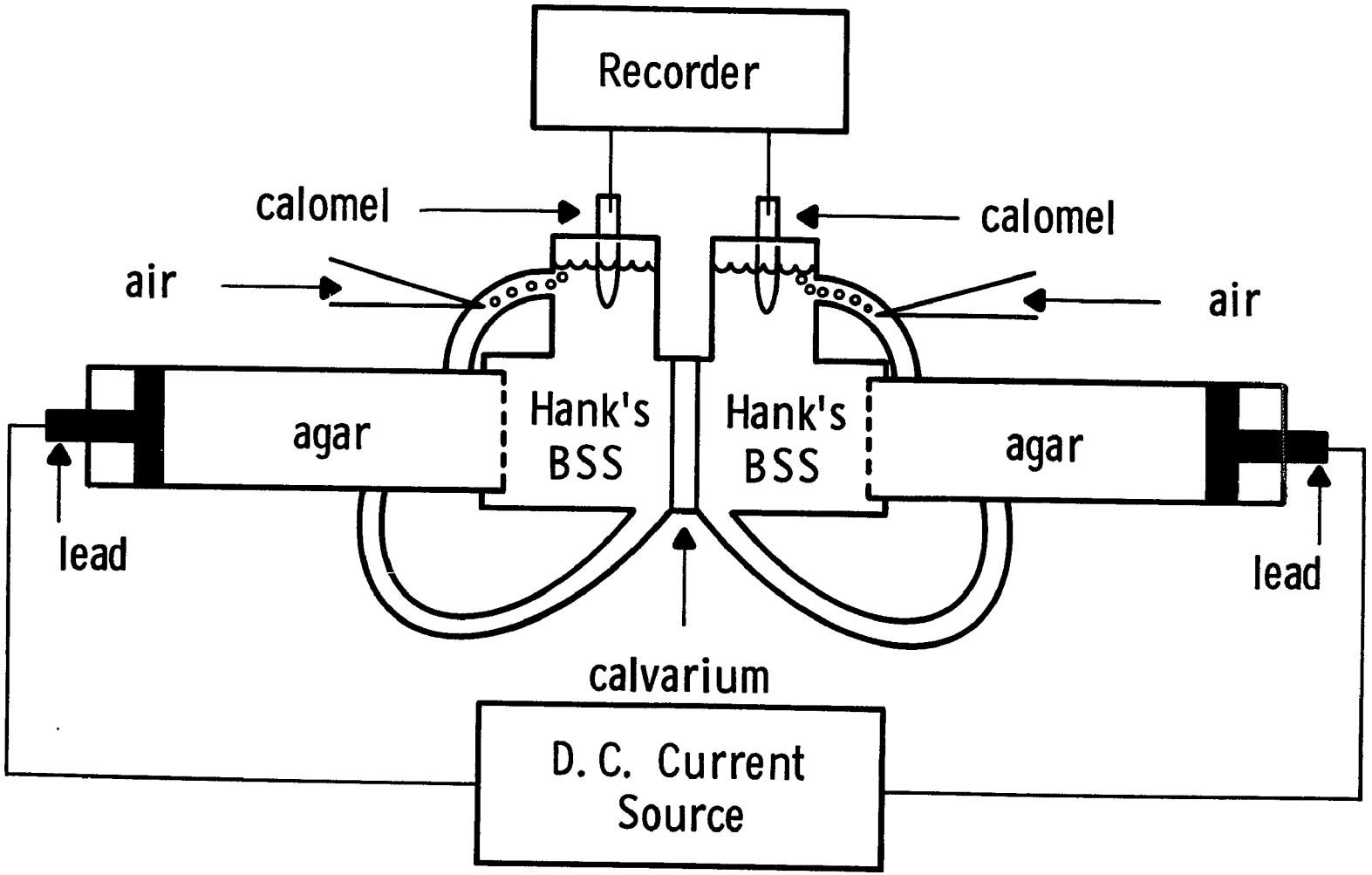
Recorder
calomel
calomel
air
air
agar
Hank's BSS
Hank's BSS
agar
lead
lead
calvarium
D. C. Current Source

Both chambers were filled with standard Hank's BSS which was recirculated by bubbling air. Each chamber contained two electrodes, a lead-lead acetate agar electrode for sending current and a calomel electrode for recording transtissue potentials. The transtissue potential was measured on a mV recorder. The current sending electrodes were used to send short (< 1 second) pulses of 10×10^{-6} amp current through the tissue. Tissue resistance was calculated from the change in transtissue potential that occurred during this pulse of current.

In four experiments the solution on the scalp (unscraped) side of the calvarium was exchanged for the constant product, chloride free, and high potassium solutions. In the other four experiments the standard solution on the scalp side was exchanged for the low sodium and calcium free solutions. The transtissue potential and resistance were measured with each solution change. Control measurements were made with standard Hank's BSS at the beginning and end of each experiment and after each solution change.

The liquid junction potential and resistance of each solution in reference to the standard Hank's BSS were measured in the same chamber without the tissue.

Results

The transtissue potential was always zero with Hank's BSS in both chambers. The resistance varied between 300 and 400 Ω so the

tissue resistance was 100 to 165 Ω cm^2. The changes of transtissue potentials and resistances observed in response to changes in the composition of the Hank's BSS on the scalp side are given in Table 9. A change to either the constant product or chloride-free solution caused a +6.0 to +7.5 mV change in transtissue potential and a 0 to 70 Ω change in resistance. The low sodium solution caused a change in potential of -2.0 to -4.0 mV and of +30 to +60 Ω in resistance. Both the high potassium and calcium-free solutions caused very small potential ($\leq$ 0.2 mV) and resistance ($\leq$ 10 Ω) changes except in experiment no. 6 where a +6.2 mV change in potential occurred with the calcium-free solution.

The junction potentials and solution resistances are not recorded in a separate table since they agreed exactly with the transtissue values given in Table 9, with the exception of the low sodium solution. The junction potential for the low sodium solution was < 1.0 mV, a much lower value than the transtissue potential recorded for the same solution.

Discussion

The results of these studies of the membrane properties of rat calvaria leave no doubt that a true bone membrane does not exist under these experimental conditions. In only one experiment was a response recorded that could not be explained by liquid junction potentials. With low sodium solutions, a transtissue potential of

Table 9. Changes in Transtissue Potential and Resistance of Calvaria in Response to Changes in Bathing Solutions

Experiment No.	Pup Age (days)	[K x Cl]		Cl-free		↑K	
		ΔP.D. (mV)*	ΔR (Ω)**	ΔP.D. (mV)	ΔR (Ω)	ΔP.D. (mV)	ΔR (Ω)
1	9	+7.0	NC	+7.5	+50	+0.2	NC
3	11	+6.0	NC	+6.0	+40	+0.1	NC
5	11	+6.0	+50	+7.0	+70	+0.1	NC
7	12	+6.5	+10	+6.0	+10	+0.2	NC

		↓Na		Ca^{++} free	
		ΔP.D. (mV)	ΔR (Ω)	ΔP.D. (mV)	ΔR (Ω)
2	10	-4.0	+60	+0.1	NC
4	11	-2.5	+30	+0.1	-10
6	11	-3.0	+60	+6.2	+10
8	12	-2.0	+85	+0.1	NC

* ΔP.D. is the change in transtissue potential observed in changing the Hank's BSS on the scalp side of the tissue to the indicated solution.

** ΔR is the change in transtissue resistance occurring simultaneously with the observed ΔP.D.

2 or 3 mV, low sodium side negative. This was not a liquid junction potential, but could reflect binding of the sodium ions (or choline substituted for sodium) to bone minerals. These same findings indicate that the calvarium as a whole is highly permeable to all ions. Without a membrane, the conclusion may be made that scraping the surface of the calvarium releases potassium from the disrupted surface cells, not from a separate bone extracellular fluid as has been proposed.

These studies do not eliminate the possibility of localized microenvironments within bone which may maintain a separate extracellular fluid.

CHAPTER 6

SUMMARY AND CONCLUSIONS

The membrane characteristics of osteoblasts *in situ* were studied on rat calvaria *in vitro*. The transmembrane potential was 4 mV, inside negative. There was no significant response of transmembrane potential to changes in external potassium, sodium, or chloride concentrations. The membrane potential variably hyperpolarized in response to calcium-free external solutions, or in response to the addition of fluoride or thyrocalcitonin to the standard external solution. The significance of these results is discussed in terms of possible membrane characteristics of osteoblast cells.

The functional significance of the morphologic cell junctions was tested by electrical and tracer studies. The cells were shown to have intercellular pathways permeable to ionic current and dye molecules. The dye movement is rapid; the electrical coupling is intermediate in magnitude when compared to cells of other tissues. The hyperpolarization observed with external fluoride and calcium ion concentration changes and with thyrocalcitonin may be significant in maintaining coupling simultaneous with high cytoplasmic calcium levels.

Studies of the membrane properties of rat calvaria as a tissue sheet between two chambers showed high permeability to all but sodium ions. This may be related to the binding of sodium to mineral crystals in the bone. Undoubtedly, the entire calvarial surface cannot maintain a separate bone extracellular fluid by any surface membrane. The reportedly high potassium content of bone must be interpreted as existing in microenvironments within bone or as of cellular origin.

The results of these studies do not completely define the membranes of bone, but the following conclusions may safely be drawn:

1) Osteoblast membranes maintain a low (4 mV), inside negative, potential. Their responses to ionic changes are inconclusive in defining the ionic origin of this potential.

2) Osteoblasts are coupled by functional cell junctions which may act in ionic and/or fluid movements in bone tissue. Hyperpolarization caused by fluoride, calcium-free, and thyrocalcitonin solutions may be significant in maintaining cell junctions in the presence of high cytoplasmic calcium levels.

3) The calvarial surface as a whole does not act as a limiting membrane to ionic fluxes. It cannot maintain ionic concentration gradients across the outer surface.

As with all research, some evidence has been given allowing certain conclusions to be drawn, but this same evidence gives rise to new questions. What is it that determines the transmembrane potential? Do the calcium regulating hormones affect osteoblast coupling? Are there localized areas of bone containing fluid high in potassium?

My interest is immediately drawn to the first two problems, whose answers may lie in an extension of the studies with ion changes and with hormonal effects on coupling.

APPENDIX 1. SOLUTIONS

A. Stock Solutions

All stock solutions were prepared from reagent grade chemicals and distilled water in the concentrations listed below:

1.00 M sodium chloride

1.00 M choline chloride

1.00 M potassium sulfate

1.00 M sodium sulfate

0.10 M glucose

0.10 M potassium chloride

0.10 M sodium bicarbonate

0.10 M magnesium sulfate

0.01 M sodium phosphate (dibasic)

0.01 M potassium phosphate (monobasic)

0.01 M calcium chloride

0.005 M sodium fluoride

B. Hank's BSS

All Hank's balanced salt solutions were prepared from the preceding stock solutions and distilled water. When necessary, the final pH of the solution was adjusted to 7.4 with 0.01 N hydrochloric

acid or 0.01 N sodium hydroxide. The final composition of each solution is listed in Table 10. The osmolarity is the calculated value.

C. TCT Hank's BSS

Porcine Calcitonin was obtained from Armour Pharmaceuticals* in a vial containing 1 mg of the lyophilized preparation. The contents of the vial were dissolved in 2 ml of 0.01 N hydrochloric acid and diluted to 4 ml with distilled water. The solution was immediately frozen in four 1 ml aliquots.

The lot of Calcitonin was assayed by the manufacturer at an average of 87.8 MRC units per vial. Thus each 1 ml aliquot contained 22 MRC units.

Just before use, one 1 ml aliquot was thawed and added to 200 ml of standard Hank's BSS. This gave a final concentration of Calcitonin of 11 MRC milliunits (mU) per ml.

D. Fluoride Hank's BSS

One ml of the stock sodium fluoride solution was added to the combined stock solution aliquots for Hank's BSS before final dilution to one liter. Thus, the final solution fluoride concentration was 0.05 mM (1 ppm).

---

*Armour Pharmaceuticals, Inc., Kankakee, Illinois.

Table 10. Composition of Hank's Balanced Salt Solutions

	Standard	Low Sodium	High Potassium	Calcium Free	Chloride Free	Constant Product
glucose	5.55*	5.55	5.55	5.55	5.55	5.55
Na^+	141.72	5.02	107.42	141.72	141.62	107.52
Cl^-	143.97	143.97	143.90	142.07	1.90	20.00
K^+	5.74	5.74	39.97	5.74	5.73	39.97
HCO_3^-	4.17	4.17	4.17	4.17	4.17	4.17
Mg^{++}	0.81	0.81	0.81	0.81	0.81	0.81
$SO_4^=$	0.81	0.81	0.81	0.81	71.79	62.31
$HPO_4^=$	0.42	0.42	0.42	0.42	0.42	0.42
$H_2PO_4^-$	0.37	0.37	0.37	0.37	0.37	0.37
Ca^{++}	0.95	0.95	0.95	--	0.95	0.95
choline	--	136.7	--	--	--	--
sucrose	--	--	--	--	71.00	61.50
mOsm	304.51	304.51	304.37	301.66	304.31	303.57

* Each value is [mM].

APPENDIX 2. HISTOLOGIC METHODS AND PROCEDURES

A. Tissue Fixation and Sectioning

All frozen sections were made 10 to 12 microns thick, from unfixed tissue. The individual sections were fixed briefly (< 2 minutes) in Bouin's solution before staining and mounting.

All tissues to be paraffin-embedded were fixed for at least 24 hours in Bouin's solution. Dehydration of the fixed tissue was performed rapidly in acidic methanol solutions: 1 hour in 70% methanol, 1 hour in 85% methanol, and 2 hours in two changes of absolute methanol. The embedded tissue sections were made 7 or 8 microns thick.

All tissues were serially sectioned. Each section was examined microscopically for the presence of the lithium carmine dye in cells.

B. Colloidal Iron Stain

1. Solutions

A stock solution of colloidal iron was prepared by adding 4.4 ml of a 29% ferric chloride solution to 250 ml of boiling water. The solution was stirred and heated until it became dark red and

clear. Then it was put in a dialysis bag and dialyzed against distilled water for two weeks.

A working solution of colloidal iron was prepared by mixing 25 ml of glacial acetic acid and 75 ml of absolute methanol into 100 ml of the stock colloidal iron solution.

A hydrochloric acid-ferrocyanide solution was prepared just before use by dissolving 2 gm of potassium ferrocyanide in 5 ml of water and adding 95 ml of absolute alcohol. To this was added 100 ml of a solution prepared by adding 2 ml hydrochloric acid to 98 ml of absolute alcohol.

2. Procedure

1) Deparaffinize paraffin-embedded sections and hydrate to 95% methanol, or dehydrate frozen sections to 95% methanol.
2) Rinse in 12% acetic acid for 30 seconds.
3) Transfer to fresh colloidal iron working solution for 60 minutes.
4) Rinse in four changes of 12% acetic acid for 3 minutes each.
5) Transfer to hydrochloridic acid-ferrocyanide solution for 20 minutes.
6) Wash in 3 changes of 95% methanol for 5 minutes each.
7) Dehydrate in absolute methanol for 15 minutes.
8) Clear in xylene and mount.

C. Toluidine Blue O Stain

1. Solution

A 1% (w/v) solution of toluidine blue O was prepared in 50% methanol.

2. Procedure

1) Deparaffinize paraffin-embedded sections and hydrate to 95% methanol, or dehydrate frozen sections to 95% methanol.
2) Dip quickly, about ½ second, in the toluidine blue O solution.
3) Dip quickly in a 3% acetic acid solution.
4) Transfer to 95% methanol until clear of blue stain (3 to 5 minutes).
5) Dehydrate in absolute methanol for 15 minutes.
6) Clear in xylene and mount.

APPENDIX 3. CABLE ANALYSIS OF THE SPREAD OF INTRACELLULARLY INJECTED CURRENT. A BESSEL FUNCTION SOLUTION (15).

Cable analysis regards the tissue as two uniform resistances, a planar resistance (R_i) to current flow within the tissue and a transverse resistance (R_z) to current flow out of the tissue (Figure 9A). The current at any distance (x) from the site of current injection within the plane is measured as a voltage (V) proportional to the resistances and distance. This proportionality is described mathematically as follows:

Consider a hollow cylindrical segment of tissue of thickness, Δx, at a radius, x, from the site of current injection (Figure 9B). For simplicity of analysis, this "washer" is unrolled and the parameters identified in Figure 9C.

By Ohm's law $$\Delta V = -I\ \Delta R \qquad (1)$$

where $$\Delta R = p\ \frac{W}{A} \qquad (2)$$

p is the specific resistance, W is the depth, and A is the surface area.

In this case, consider the flow of current within the tissue of specific resistance R_i. Here the depth is Δx and the area is $2\pi xL$ where L is the tissue thickness.

Substituting, $$\Delta V = -I\ R_i\ \frac{\Delta x}{2\pi xL} \qquad (3)$$

then $$\frac{dV}{dx} = \frac{-I\ R_i}{2\pi xL} \qquad (4)$$

Figure 9. Geometric and Mathematical Representation of the Tissue as Used in Bessel Function Analysis of Current Spread. (A) Side view of tissue with the microelectrode injecting current, I_o. The tissue is two uniform resistances: R_i, a planar resistance, and R_z, a transverse (cell membrane) resistance. (B) Instantaneous analysis of current some time after current injection. Current has traveled a distance of x microns and is localized in a small washer-like segment, Δx. Cell thickness is L. (C) The "washer" is unrolled to show the surface dimensions. The washer is Δx by $2\pi x$ by L.

(A)

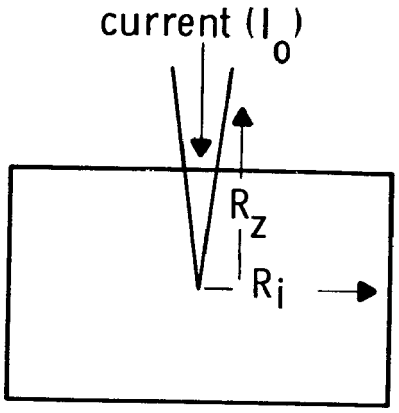

(B)

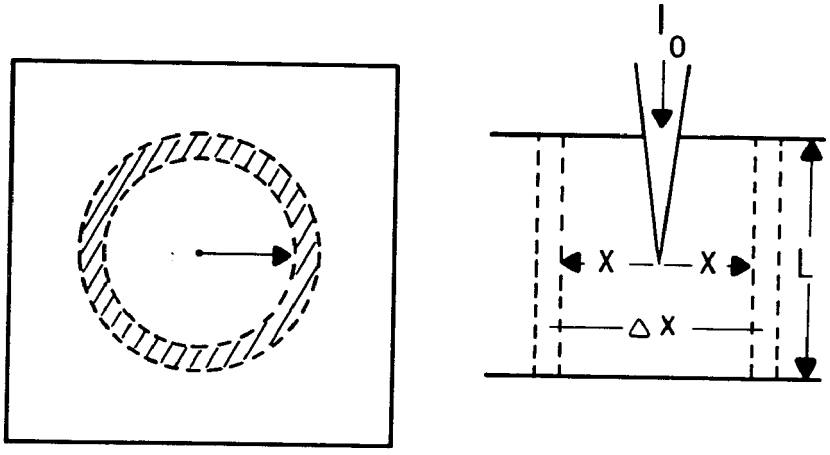

(C)

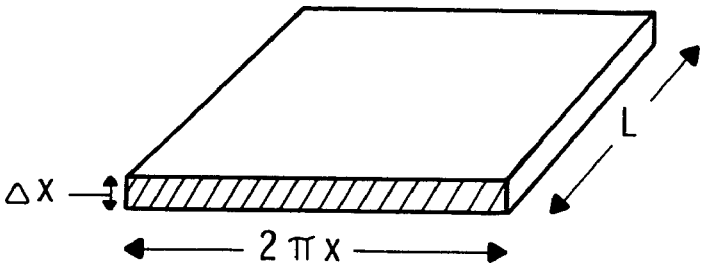

and $$\frac{d^2V}{dx^2} = \frac{-R_i}{2\pi xL} \frac{dI}{dx} + \frac{R_i I}{2\pi x^2 L} \quad (5)$$

However, I is not constant since it is also diminished by the amount lost from the tissue through the transverse resistance R_z. The change in current, ΔI, is described by the equation

$$\Delta I = -\frac{V}{\Delta R} \quad (6)$$

where R is defined by equation (2). But here $R_z = pW$, W is the cell membrane thickness (considered finite but very small compared to x and Δx), and A is $2\pi x\, \Delta x$.

Thus, $$\Delta I = -\frac{V}{\frac{R_z}{2\pi x\, \Delta x}} \quad (7)$$

or $$\Delta I = -\frac{V\, 2\pi x\, \Delta x}{R_z} \quad (8)$$

then $$\frac{dI}{dx} = -\frac{V\, 2\pi x}{R_z} \quad (9)$$

Rearrangement of equation (5) yields

$$I = -\frac{2\pi xL}{R_i} \frac{dV}{dx} \quad (10)$$

Substitution of equations (9) and (10) into equation (5) yields

$$\frac{d^2V}{dx^2} = -\frac{R_i}{2\pi xL}\left[-\frac{V\, 2\pi x}{R_z}\right] + \frac{R_i}{2\pi x^2 L}\left[-\frac{2\pi xL}{R_i} \frac{dV}{dx}\right]$$

or $$\frac{d^2V}{dx^2} + \frac{1}{x} \frac{dV}{dx} - V\left[\frac{R_i}{L\, R_z}\right] = 0 \quad (11)$$

We define $$\lambda^2 \equiv \frac{L\, R_z}{R_i} \quad (12)$$

Then $$\frac{d^2V}{dx^2} + \frac{1}{x}\frac{dv}{dx} - \frac{V}{\lambda^2} = 0 \qquad (13)$$

This is a second order differential equation describing the voltage as a function of distance from the site of current injection. Its solution is

$$V = A\, K_o \left[\frac{x}{\lambda}\right] \qquad (14)$$

where $$A = \frac{I_o\, R_i}{2\pi L} \qquad (15)$$

and K_o is the zero order modified Bessel function of the second kind and I_o is the injected current.

From equations (12) and (15) we can also obtain

$$R_z = \frac{2\pi A \lambda^2}{I_o} \qquad (16)$$

and $$\frac{R_i}{L} = \frac{2\pi A}{I_o} \qquad (17)$$

Experimentally, a set of distances and voltages are obtained in response to a constant injected current. These are fitted to the solution (equation (14) above) by adjustment of A and λ to give a best fit by the least squares technique. A computer program was made to do this, and to solve for R_z and R_i.

REFERENCES

1. Adrian, E. D., and Moruzzi, G. Impulses in the Pyramidal Tract. J. Physiol. 97: 153-199, 1939.

2. Baud, C. A. Submicroscopic Structure and Functional Aspects of the Osteocyte. Clin. Orthop. 56: 227-236, 1968.

3. Bennett, M. V. L. Function of Electrotonic Junctions in Embryonic and Adult Tissues. Fed. Proc. 32: 65-75, 1973.

4. Bonucci, E. The Locus of Initial Calcification in Cartilage and Bone. Clin. Orthop. 78: 108-139, 1971.

5. Borle, A. B. Effects of Purified Parathyroid Hormone on the Calcium Metabolism of Monkey Kidney Cells. Endocrinology 83: 1316-1322, 1968.

6. Borle, A. B. Kinetic Analyses of Calcium Movements in HeLa Cell Cultures. I. Calcium Influx. J. Gen. Physiol. 53: 43-56, 1969.

7. Borle, A. B. Kinetic Analyses of Calcium Movements in HeLa Cell Cultures. II. Calcium Efflux. J. Gen. Physiol. 53: 57-69, 1969.

8. Borle, A. B. Effects of Thyrocalcitonin on Calcium Transport in Kidney Cells. Endocrinology 85: 194-199, 1969.

9. Borle, A. B. Kinetic Analysis of Calcium Movements in Cell Culture. V. Intracellular Calcium Distribution in Kidney Cells. J. Membrane Biol. 10(1): 45-66, 1972.

10. Canas, F., Terepka, A. R., and Neuman, W. F. Potassium and the Milieu Interieur of Bone. Am. J. Physiol. 217: 117-120, 1969.

11. Cole, K. S., and Curtis, H. J. Electric Impedance of the Squid Giant Axon During Activity. J. Gen. Physiol. 22: 649-670, 1939.

12. Davis, T. L., Jackson, J. W., Day, B. E., Shoemaker, R. L., and Rehm, W. S. Potentials in Frog Cornea and Microelectrode Artifact. Am. J. Physiol. 219: 178-183, 1970.

13. Davson, H. A Textbook of General Physiology, Fourth edition, pp. 462-463 and 548-558. Baltimore: The Williams and Wilkins Company, 1970.

14. DeLuca, H. F., and Engstrom, G. W. Calcium Uptake by Rat Kidney Mitochondria. Proc. Natn. Acad. Sci. USA 47: 1744-1750, 1961.

15. Fromter, E., and Diamond, J. Route of Passive Ion Permeation in Epithelia. Nature New Biol. 235: 9-13, 1972.

16. Geisler, J. Z., and Neuman, W. F. The Membrane Control of Bone Potassium. Proc. Soc. Exp. Biol. Med. 130: 608-612, 1969.

17. Hodgkin, A. L., and Huxley, A. F. Action Potentials Recorded from Inside a Nerve Fiber. Nature 144: 710-711, 1939.

18. Holtrop, M. E., and Weinger, J. M. "Ultrastructural Evidence for a Transport System in Bone". In Calcium, Parathyroid Hormone and the Calcitonins, ed. by Talmage and Munson, pp. 365-374. Amsterdam: Excerpta Medica Foundation, 1972.

19. Howard, J. E. "Present Knowledge of Parathyroid Function, with Special Emphasis Upon Its Limitations". In Ciba Foundation Symposium on Bone Structure and Metabolism, ed. by Walstenholme and O'Conner, pp. 206-221. Boston: Little, Brown and Company, 1959.

20. Irving, J. T., and Wuthier, R. E. Histochemistry and Biochemistry of Calcification with Special Reference to the Role of Lipids. Clin. Orthop. 56: 237-260, 1968.

21. Kanno, Y., and Loewenstein, W. R. Low Resistance Coupling Between Gland Cells. Some Observations on Intracellular Contact Membranes and Intercellular Space. Nature 201: 194-195, 1964.

22. Kravitz, E. A., Stretton, A. O. W., Alvarez, J., and Furshpan, E. J. Determination of Neuronal Geometry Using an Intracellular Dye Injection Technique. Fed. Proc. 27: 749, 1968.

23. Lehninger, A. L. Mitochondria and Calcium Ion Transport. Biochem. J. 119: 129-138, 1970.

24. Lillie, R. D. H. J. Conn's Biological Stains, Eighth edition, p. 335. Baltimore: The Williams and Wilkins Company, 1969.

25. Ling, G., and Gerard, R. W. The Normal Membrane Potential of Frog Sartorius Fibers. J. Cell and Comp. Physiol. 34: 383-396, 1949.

26. Loewenstein, W. R., and Kanno, Y. Studies on an Epithelial (Gland) Cell Junction. I. Modifications of Surface Membrane Permeability. J. Cell Biol. 22: 565-586, 1964.

27. Loewenstein, W. R., Nakas, M., and Socolar, S. J. Junctional Membrane Coupling. Permeability Transformations at a Cell Membrane Junction. J. Gen. Physiol. 50: 1865-1891, 1967.

28. Loewenstein, W. R., Socolar, S. J., Higashino, S., Kanno, Y., and Davidson, N. Intercellular Communication: Renal, Urinary Bladder, Sensory, and Salivary Gland Cells. Science 149: 295-298, 1965.

29. Mears, D. C. Effects of Parathyroid Hormone and Thyrocalcitonin on the Membrane Potential of Osteoclasts. Endocrinology 88: 1021-1028, 1971.

30. Neuman, W. F., and Neuman, M. W. The Chemical Dynamics of Bone Mineral. Chicago: University of Chicago Press, 1958.

31. Neuman, W. F., Terepka, A. R., Canas, R., and Triffit, J. T. The Cycling Concept of Exchange in Bone. Calc. Tiss. Res. 2: 262-270, 1968.

32. Oikawa, T., Ogawa, T., and Motokawa, K. Origin of So-called Cone Action Potential. J. Neurophysiol. 22: 102-111, 1959.

33. Oliveira-Castro, G. M., and Loewenstein, W. R. Junctional Membrane Permeability. Effects of Divalent Cations. J. Membrane Biol. 5: 51-77, 1971.

34. Park, H. Z., and Talmage, R. V. Relation of Endogenous Parathyroid Secretion to ^{3}H-cytidine Incorporation into Bone Cells. Endocrinology 80: 552-560, 1967.

35. Park, H. Z., and Talmage, R. V. "Comparison of the Effects of Calcium and Endogenous Parathyroid Hormone on RNA Synthesis in Bone". In Parathyroid Hormone and Thyrocalcitonin (Calcitonin), ed. by Talmage and Belanger, pp. 203-215. Amsterdam: Excerpta Medica Foundation, 1968.

36. Paul, J. Cell and Tissue Culture, Third edition, p. 83. Baltimore: The Williams and Wilkins Company, 1965.

37. Rasmussen, H., Feinblatt, J., Nagata, N., and Pechet, M. Effect of Ions Upon Bone Cell Function. Fed. Proc. 29(3): 1190-1197, 1970.

38. Rehm, W. S. Acid Secretion, Resistance, Short Circuit Current, and Voltage-clamping in Forg's Stomach. Am. J. Physiol. 203: 63-72, 1962.

39. Rehm, W. S., and Enelow, A. J. A Study of the Alleged Effect of Milk on the Human Gastric Potential and a Description of a New Method for Measuring the Potential. Gastroenterology 3: 306-313, 1944.

40. Sachs, G., Shoemaker, R. L., Blum, A. L., Helander, H. F., Maklouf, G. M., and Hirschowitz, B. I. "Microelectrode Studies of Gastric Mucosa and Isolated Gastric Cells". In Electrophysiology of Epithelial Cells, ed. by G. Giebisch, pp. 257-279. New York: Symposia Medica Hoescht/F. K. Schattauer Verlag, 1970.

41. Shoemaker, R. L., Maklouf, G. M., and Sachs, G. Action of Cholinergic Drugs on Necturus Gastric Mucosa. Am. J. Physiol. 219: 1056-1060, 1970.

42. Talmage, R. V. Parathyroid Function: A Calcium Replacement Mechanism. Amer. Zool. 2: 353-360, 1963.

43. Talmage, R. V. Calcium Homeostasis - Calcium Transport - Parathyroid Action. Clin. Orthop. 67: 211-223, 1969.

44. Tomita, T., Murakami, M., Sato, Y., and Hashimoto, Y. Further Study on the Origin of the So-called Cone Action Potential (S-Potential). Its Histological Determination. Japan J. Physiol. 9: 63-68, 1959.

45. Triffit, J. T., Terepka, A. R., and Neuman, W. F. A Comparative Study of the Exchange in Vivo of Major Constituents of Bone Mineral. Calc. Tiss. Res. 2: 165-176, 1968.

46. Villegas, L. Cellular Location of the Electrical Potential Difference in Frog Gastric Mucosa. Biochim. Biophys. Acta 64: 359-367, 1962.

47. Vitalli, P. H. Osteocyte Activity. Clin. Orthop. 56: 213-226, 1968.

48. Whitson, S. W. Tight Junction Formation in the Osteon. Clin. Orthop. 86: 206-213, 1972.

49. Winter, H. F., Bishop, J. G., and Dorman, H. L. Transmembrane Potentials of Odontoblasts. J. Dent. Res. 42: 594-598, 1963.

GRADUATE SCHOOL
UNIVERSITY OF ALABAMA IN BIRMINGHAM
DISSERTATION APPROVAL FORM

Name of Candidate Billie Gail Griggs Jeansonne

Major Subject Physiology and Biophysics

Title of Dissertation Electrophysiologic Studies of Osteoblasts

Dissertation Committee:

Frederick F. Keagen, Chairman
Donald R. Kegler
Warren S. Rehm
Jean K. Schneyer
Richard L. Thurmond
Thomas W Feaney

Director of Graduate Program Warren S. Rehm

Dean, UAB Graduate School S B Barker

Date 1 June 1973